Cold molecular ions in traps: methods and applications
Lecture II

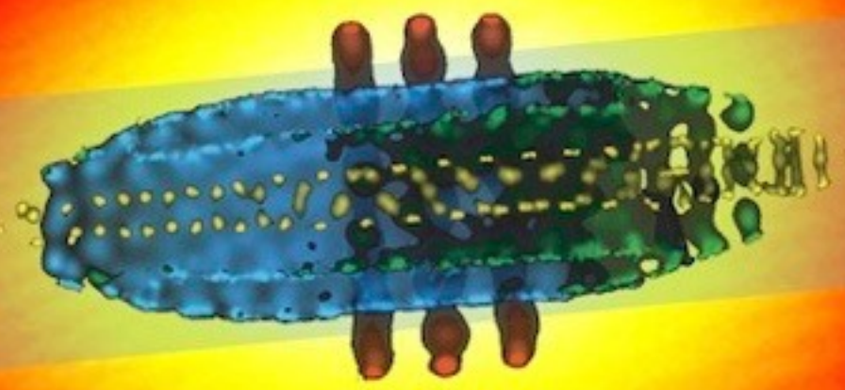

TIFR-ICTS Online School and Discussion
Meeting on Trapped Atoms, Molecules and Ions
May 10-22, 2021

Stefan Willitsch
Department of Chemistry
University of Basel, Switzerland

Contents

Lecture I
Cold molecular ions: Basic techniques and spectroscopy

1. Cooling and trapping of molecular ions: basic techniques
2. Internal-state preparation of cold molecular ions
3. Precision spectroscopy of cold molecular ions
4. Molecular-ion quantum technologies and quantum-logic spectroscopy

Lecture II
Cold ion-neutral interactions

5. Ion-neutral interactions: theory
6. Ion-atom hybrid systems
7. Molecular ions in hybrid traps

5. Ion-neutral interactions: theory

Elements of classical collision theory

- **Types of collision events:**
  - **Elastic collisions:** total kinetic energy and the internal state of the collision partners are conserved
  - **Inelastic collisions:** total kinetic energy and internal state of the reaction partners change, the chemical structure is conserved
  - **Reactive collisions:** kinetic energy, internal state and chemical structure change

Elastic collisions

- Elastic collisions, i.e., collisions in which the kinetic energy is conserved, are the simplest form of scattering events.
- Consider the collision trajectory of two structureless particles (e.g., atoms) in the centre-of-mass (COM) frame:
- As the total angular momentum is conserved, two coordinates suffice to describe the relative motion of the collision partners. We choose

R ... relative position vector
ψ ... orientation angle of R with respect to the original velocity vector v

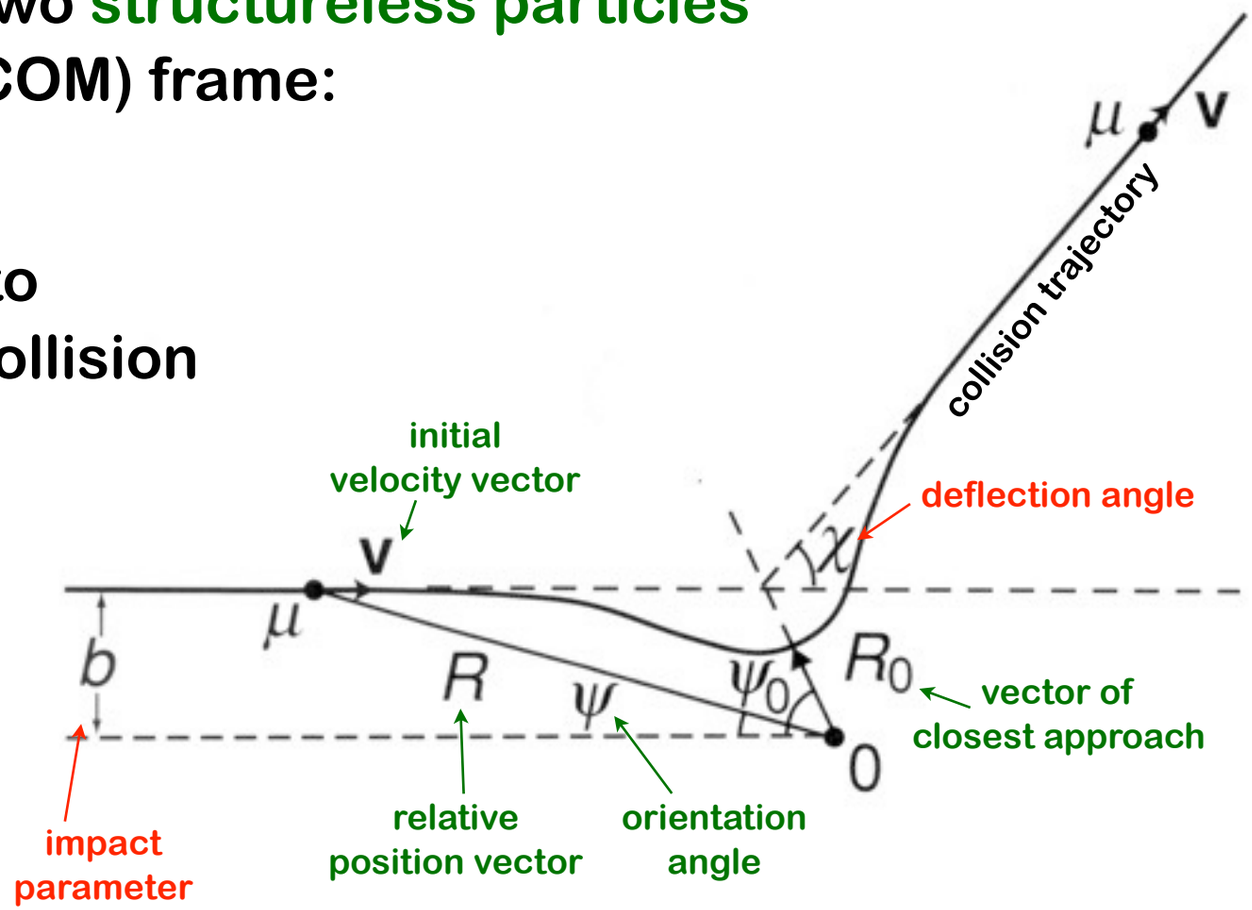

Relevant physical quantities

Angular momentum: $\vec{L} = \mu\vec{v} \times \vec{R}$

L before collision = L after collision:

$|\vec{L}| = L = |\mu\vec{v} \times \vec{R}|$ **where μ is the reduced mass**

$= \mu\vec{v} \cdot \vec{R} \sin\Psi$

$$|\vec{L}| = L = \mu v b$$

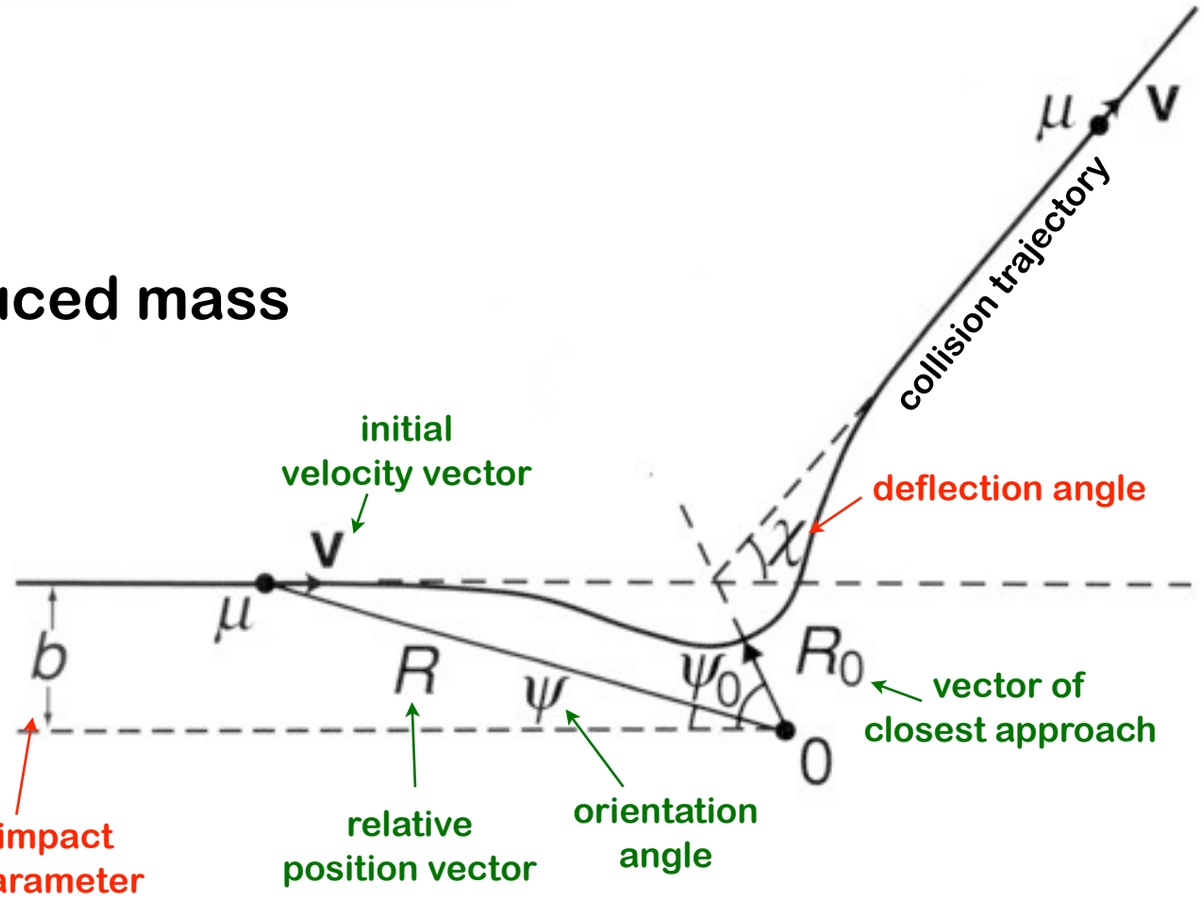

Total energy:

$$E = E_{kin} + E_{cent} + E_{pot}$$

kinetic centrifugal potential

$$= \frac{1}{2}\mu\dot{R}^2 + \frac{1}{2}\mu R^2\dot{\psi}^2 + V(R)$$ **with the angular velocity** $\dot{\psi} = d\Psi/dt = \omega$

$$= \frac{1}{2}\mu\dot{R}^2 + \frac{1}{2}\frac{L^2}{\mu R^2} + V(R) \quad \Rightarrow E = \frac{1}{2}\mu\dot{R}^2 + \frac{1}{2}\frac{L^2}{\mu R^2} + V(R)$$

$L = \mu R^2\omega$

$V_L(R)$ ... centrifugally corrected (effective) potential

- **Collision cross section (hard-sphere approximation):**

$$\sigma = \pi b_{\max}^2$$

with b_{max} … maximum impact parameter

- **Collision rate constant:** $k = \sigma v$

Centrifugally corrected potentials

- **Centrifugal energy = energy taken up in the rotation of the position vector R**
- **Collisional angular momentum L = angular momentum associated with the rotation of R about ψ**
- **The effective potential for the collision contains both, the interaction potential V(R) and the centrifugal energy:**

$$V_L(R) = \frac{1}{2}\frac{L^2}{\mu R^2} + V(R)$$

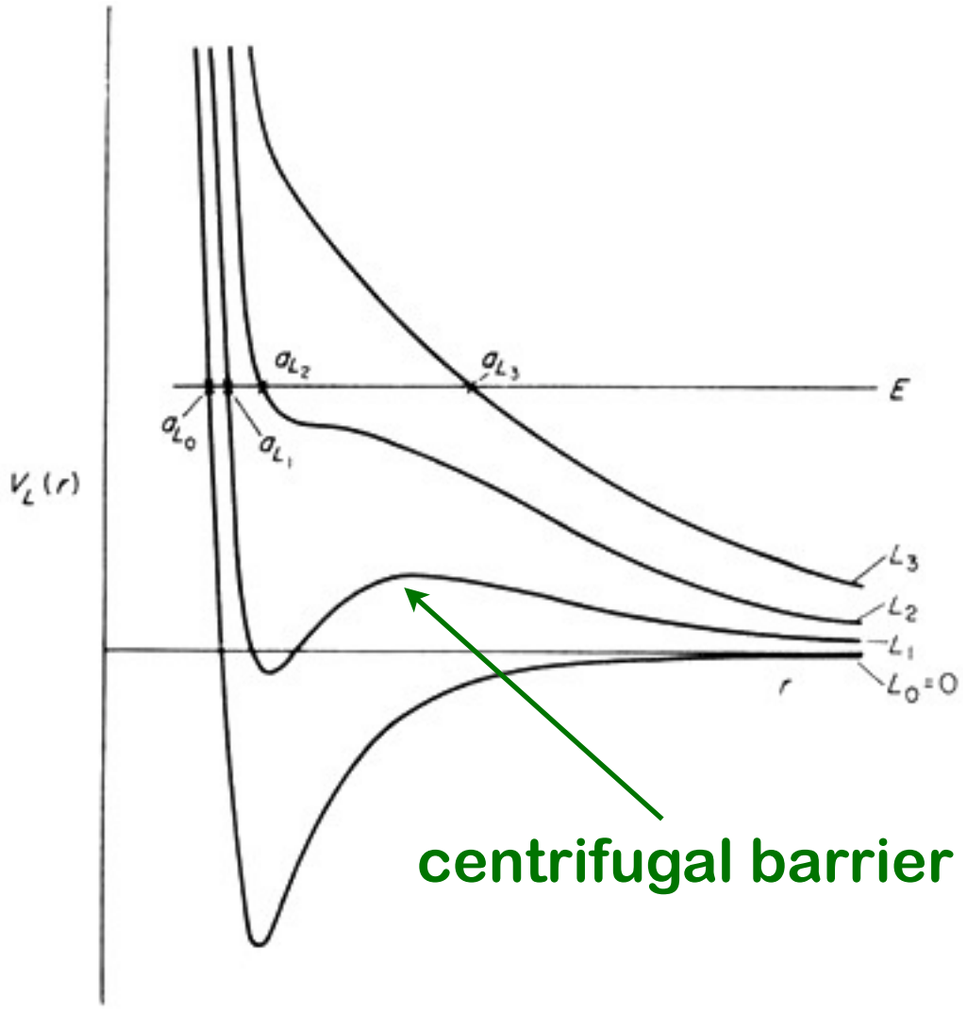

Centrifugally corrected potentials
$V_L(R)$ for $L_3 > L_2 > L_1 > L_0=0$

Ion-neutral long-range interactions

Lit.: e.g., A. Osterwalder, O. Dulieu (ed.), Cold Chemistry, RSC Publishing, 2018;
M. Tomza et al., Rev. Mod. Phys. 91 (2019), 035001

- **Ion-neutral interactions are governed by the long-range part of the interaction potential which is usually expressed as a power series in the internuclear distance R:**

$$V(R) = \frac{C_2}{R^2} + \frac{C_3}{R^3} + \frac{C_4}{R_4} + \ldots$$

- **The C_2 term corresponds to the charge-dipole interaction with**

dipole moment of the neutral molecule; orientation angle of the charge w.r.t. the dipole

$$C_2 = -\frac{\mu_D \cos\theta}{R^2}$$ **(in atomic units)**

This is usually the leading term if the neutral interaction partner is a polar neutral molecule (it is zero for apolar neutrals and neutral atoms)

- **The C_3 term is the ion-quadrupole interaction. This is usually the leading term if the neutral interaction partner is an atom in a P,D,F,... state or an apolar molecule. If the neutral is a linear molecule with quadrupole moment Q, we have**

quadrupole moment of the neutral molecule; orientation angle of the charge w.r.t. the molecular axis

$$C_3 = \frac{Q(3\cos^2\theta - 1)}{2R^3}$$ **(in atomic units)**

If the neutral interaction partner is an atom in a P,D,F,... state, the C_3 coefficient is more conveniently expressed as

$$C_3 = (-1)^{1+L-\Lambda} \begin{pmatrix} L & 2 & L \\ -\Lambda & 0 & \Lambda \end{pmatrix} \langle \varphi || Q_2 || \varphi \rangle$$

(in atomic units)

electronic orbital angular momentum (L) and projection (Λ) quantum number

Wigner 3j symbol

reduced matrix element of the quadrupole moment Q_2

- The C_4 term is the ion-induced dipole (Langevin) interaction with

$$C_4 = -\tfrac{1}{2}\alpha$$

scalar polarisability of the neutral

(in atomic units)

This is the leading term if the neutral is a structureless polarisable particle, i.e., an atom in an S state or an apolar molecule with small quadrupole moment. Usually, the C_4 coefficient also has an anisotropic component because the neutral is not structureless.

Capture processes

Lit: A. Osterwalder, O. Dulieu (ed.), Cold Chemistry, RSC Publishing, 2018

- Ion-neutral collisions are often dominated by capture dynamics. This means that the collision rate is entirely determined by the long-range attractive interactions between the reaction partner.
- Important example: Langevin capture
- If there are no other energetic barriers along the collision coordinate, the centrifugal barrier constitutes the limiting factor. Classically, a successful collision event can only happen if the collision energy E_c exceeds the height of the barrier.

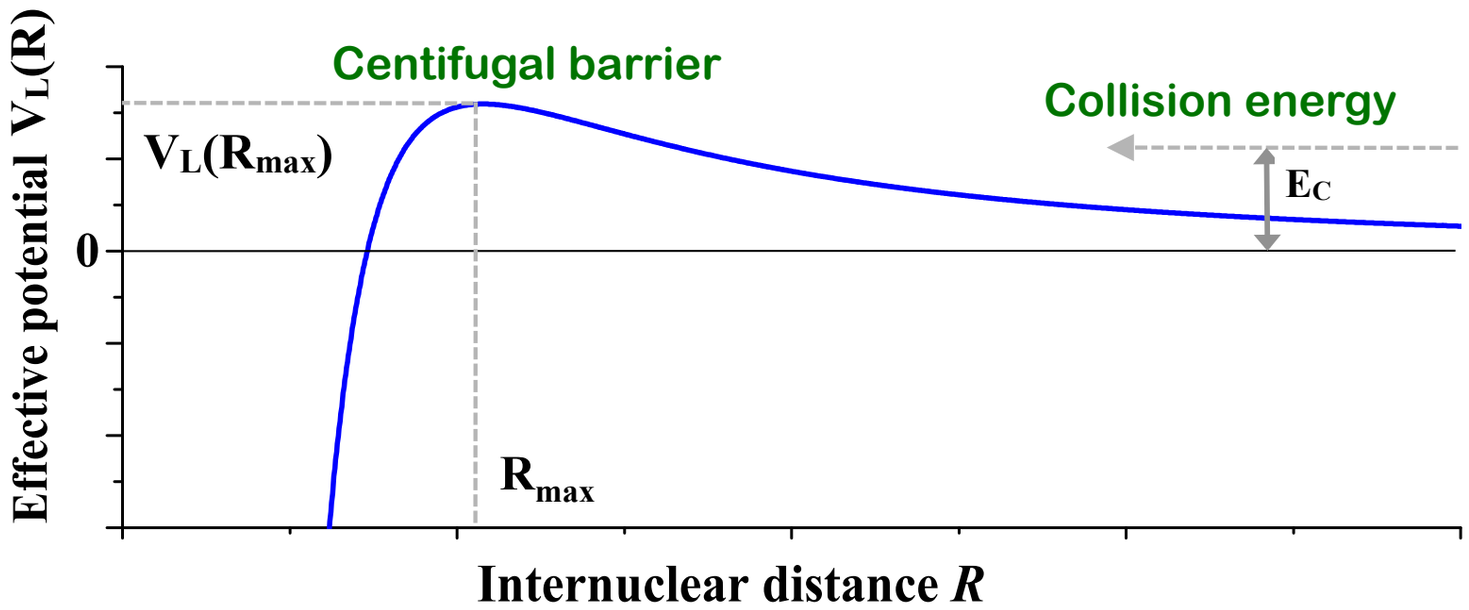

- The effective potential $V_L(R)$ and hence the height of the centrifugal barrier depend on the collisional angular momentum L:

$$V_L(R) = \frac{1}{2}\frac{L^2}{\mu R^2} + V(R)$$

- The collisional angular momentum in turn depends on the impact parameter b:

$$|\vec{L}| = L = \mu v b$$

- **Hence, for a specific collision energy E_c, there is a maximum collisional angular momentum L_{max} with impact paramter b_{max} which fulfils the condition:**

$$V_L(b_{\max}) = E_c$$

The collisional cross section is hence calculated as:

$$\sigma = \pi b_{\max}^2$$

yielding a corresponding rate constant for the collision:

$$k = \sigma v(E_c)$$

where $v(E_c) = \sqrt{2E_c/\mu}$ **is the collision velocity at energy E_c.**

- **Ion-neutral collisions often (at least approximately) fulfil classical capture dynamics as outlined above in the classical collision regime. If the long-range potential is dominated by the ion-induced dipole ("Langevin") interaction**

$$V(R) = -\frac{1}{2}\frac{\alpha' e^2}{4\pi\varepsilon_0}\frac{1}{R^4}$$

α'=α/4πε₀ ... polarisability volume of the neutral
e ... elementary charge

(in SI units)

one obtains from the conditions above the Langevin collision cross section and rate constant:

$$\sigma = \pi\sqrt{\frac{\alpha' e^2}{2\pi\varepsilon_0 E_c}} \qquad k = \sqrt{\frac{\pi\alpha' e^2}{\varepsilon_0\mu}}$$

Please mind: the Langevin rate constant is independent of the collision energy and, therefore, of temperature !

Outline of quantum elastic-collision theory

Lit.: e.g., M.S. Child, Molecular Collision Theory, Dover 1996; R.V. Krems, Molecules in Electromagnetic Fields, Wiley 2019; A. Osterwalder, O. Dulieu (ed.), Cold Chemistry, RSC Publishing, 2018

- **The quantum-mechanical problem of the elastic scattering of two structureless particles reduces to solving the time-independent scattering Schrödinger eq. for positive energies E:**

collisional angular momentum operator

$$\left[-\frac{\hbar^2}{2\mu}\frac{1}{R}\frac{\partial^2}{\partial R^2}R + \frac{\hat{L}^2}{2\mu R^2} + V(\vec{R}) \right] \Psi(\vec{R}) = E\Psi(\vec{R})$$

- **The Schrödinger eq. has the general solution:**

$$\Psi_L(\vec{R}) = \frac{1}{R}\varphi_L(R)P_L(\cos\theta)$$

Legendre polynomial of order L

with the collisional angular momentum quantum number L=0,1,2,...

- **The radial scattering wave functions $\varphi_L(R)$ have the asymptotic form**

$$\varphi_L(R \to \infty) \approx \sin\left(kR - L\pi/2 + \eta_L\right)$$

Scattering phase

where $k = \sqrt{2\mu E}/\hbar$ **... wave number of the collision (E=collision energy, μ=reduced mass)**

- **The scattering cross section is given by**

$$\sigma = \frac{4\pi}{k^2} \sum_{L=0}^{\infty} (2L+1) \sin^2 \eta_L$$

- **In the semi-classical limit (large L), the scattering phase shift η_L for elastic collisions can be approximated by**

$$\eta_L \approx \frac{\pi \mu C_4}{4\hbar^4} \frac{E}{L^3}$$

- **This leads to a semi-classical expression for the elastic scattering cross section:**

$$\sigma = \pi \left(\frac{\mu C_4}{\hbar^2}\right)^{1/3} \left(1 + \frac{\pi^2}{16}\right) E^{-1/3}$$

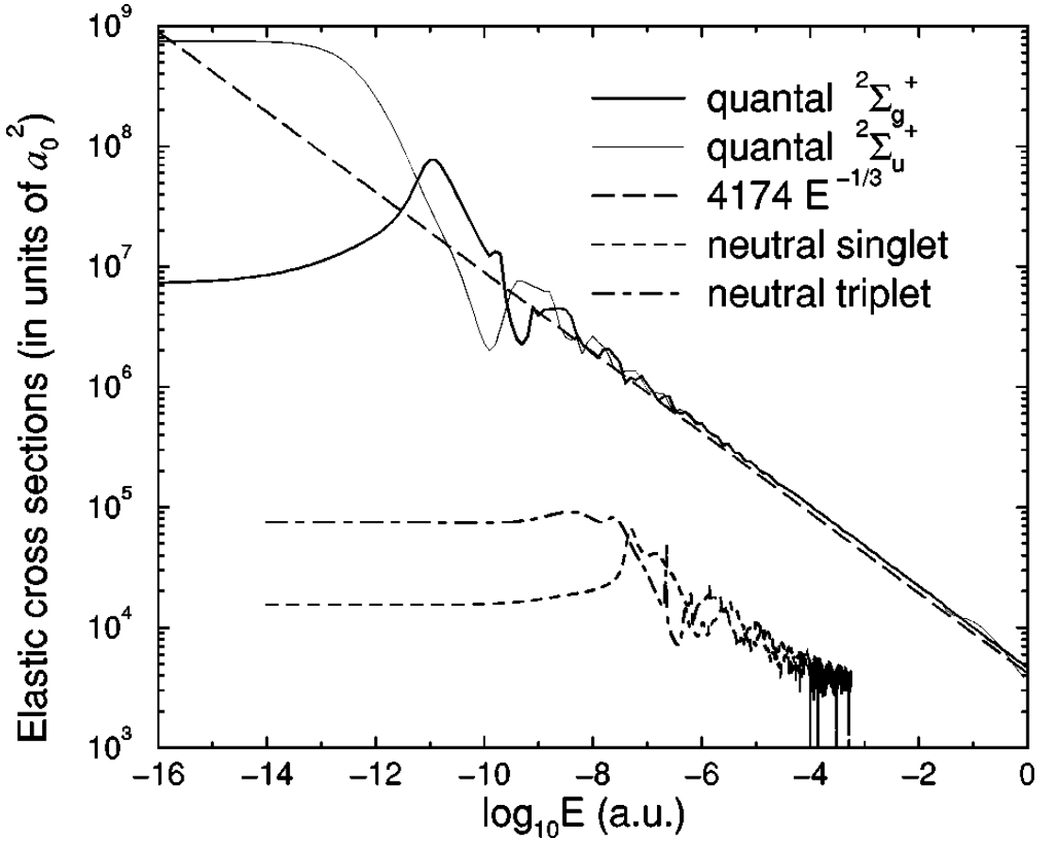

Na^+ + Na elastic collision cross sections

R. Cote and A. Dalgarno, PRA 62 (2000), 012709

6. Ion-atom hybrid systems

- **Hybrid trap:** combined ion-atom trap (first proposed by R. Cote, W.W. Smith, early 2000s)

  W.W. Smith et al., J. Mod. Opt. 52 (2005), 2253

- **Implementations:**

  - Surface-electrode ion trap with MOT

    A.T. Grier et al., PRL 102 (2009), 223201

  - Linear Paul trap with MOT

    F. Hall et al., PRL 107 (2011), 043202; PRL 109 (2012), 233202
    W. Rellergert et al., PRL 107 (2011), 243201
    K. Ravi et al., Nat. Commun. 3 (2012), 1126
    I. Sivarajah et al., PRA 86 (2012), 063419
    S. Haze et al., PRA 87 (2013), 052715
    S. Jyothi et al., RSI 90 (2019), 103201

  - Linear Paul trap with magnetic trap and/or optical dipole trap for atoms in a BEC

    C. Zipkes et al., Nature 464 (2010), 388
    S. Schmid et al., PRL 105 (2010), 133202
    Z. Meir et al., PRL 117 (2016), 243401
    J. Joger et al., PRA 96 (2017), 030703

Reviews:
- M. Tomza et al., Rev. Mod. Phys. 91 (2019), 035001
- A. Härter, J. Hecker Denschlag, Contemp. Phys. 55 (2014), 33
- S. Willitsch, Proc. Int. Sch. Phys. Enrico Fermi 189 (2015), 255
- C. Cias, M. Köhl, in "Quantum Gas Experiments", World Scientific 2014

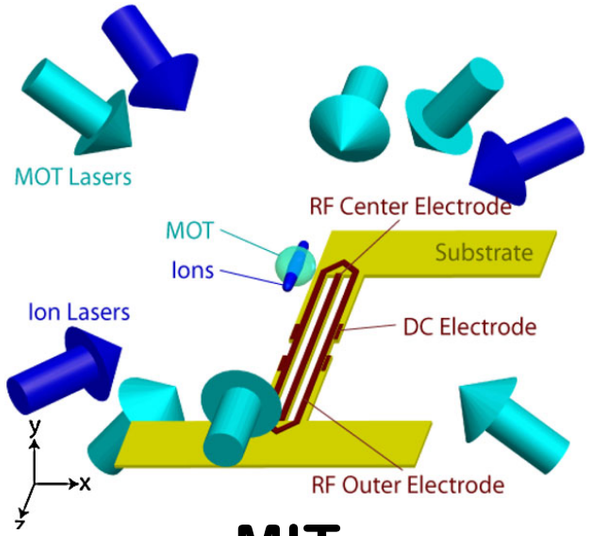

MIT

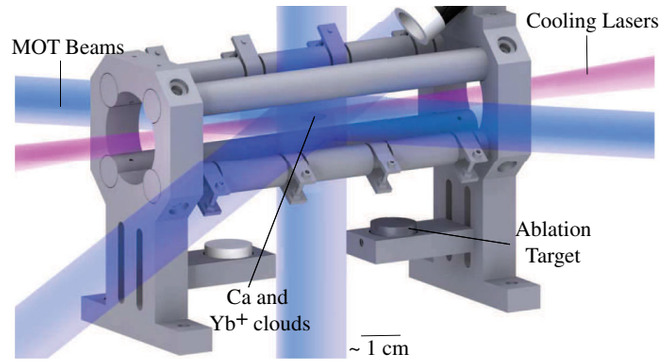

UCLA

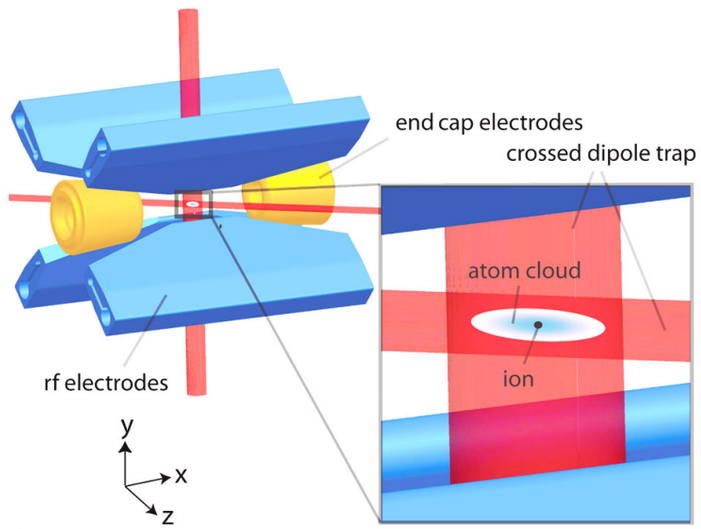

U. Ulm

Example: the Basel hybrid-trap experiment:

F.H.J. Hall et al., Phys. Rev. Lett. 107 (2011), 243202; Mol. Phys. 111 (2013), 2020

- Rb MOT superimposed on atomic/molecular Coulomb crystal in a linear Paul trap
- Tailored for collision experiments between cold atoms and atomic or molecular ions down to mK energies

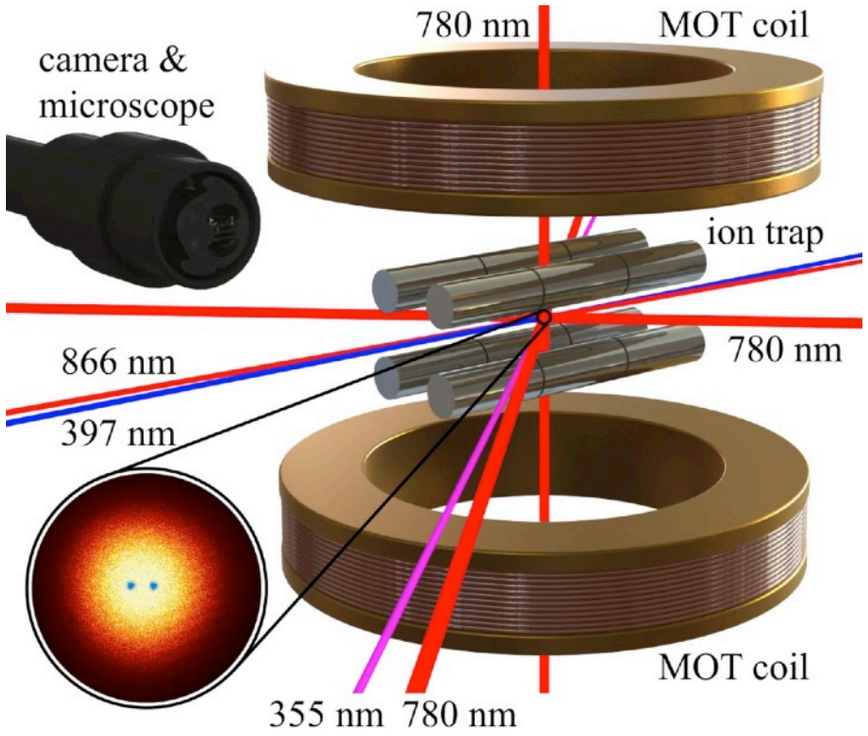

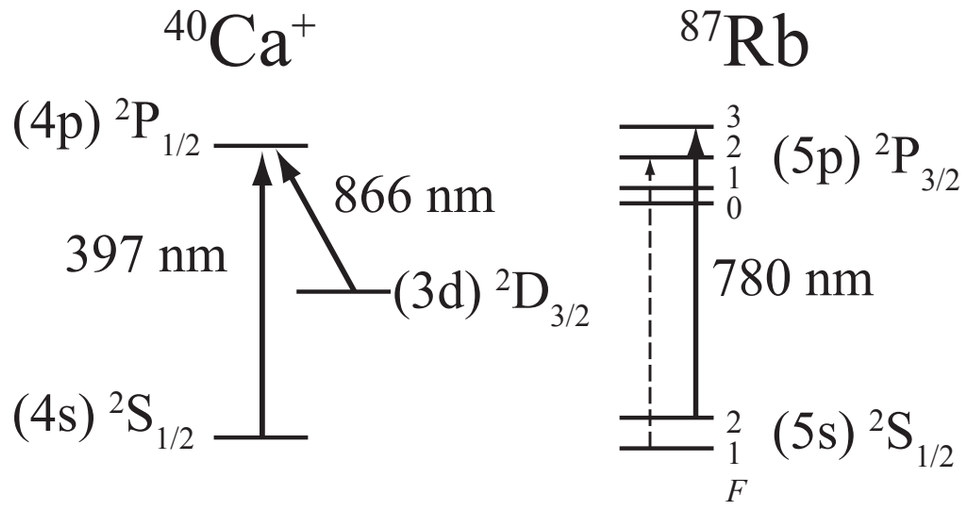

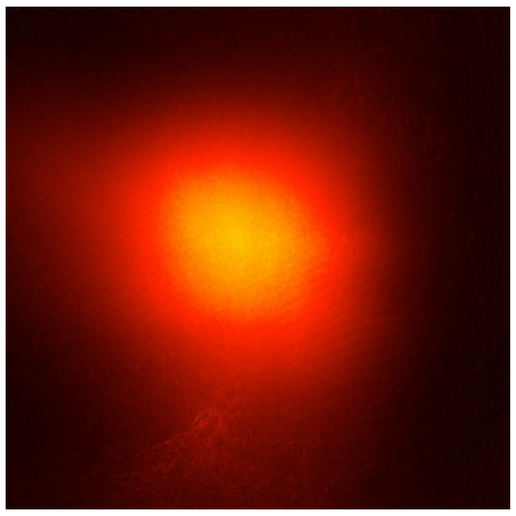

MOT

- Atom: Rb
- Number of atoms: N≈10^5-10^6
- Density: n≈10^8-10^{10} cm^{-3}
- Atom temperature: T>100 μK

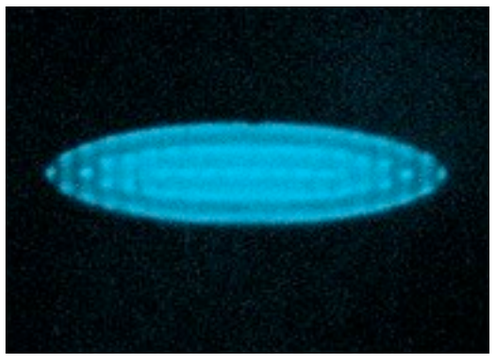

Ion trap

- Ion: Ca^+ (Ba^+), molecular ions
- Number of ions: N≈1-1000
- Density: n≈10^8 cm^{-3}
- Ion temperature (secular): T>5 mK

Cold elastic ion-atom collisions

- Elastic collisions between the ions and the atoms typically transfer micromotion energy to the atoms, leading to their loss from the trap:

Trap loss of Rb atoms by collisions with Ba^+ and Rb^+ ions

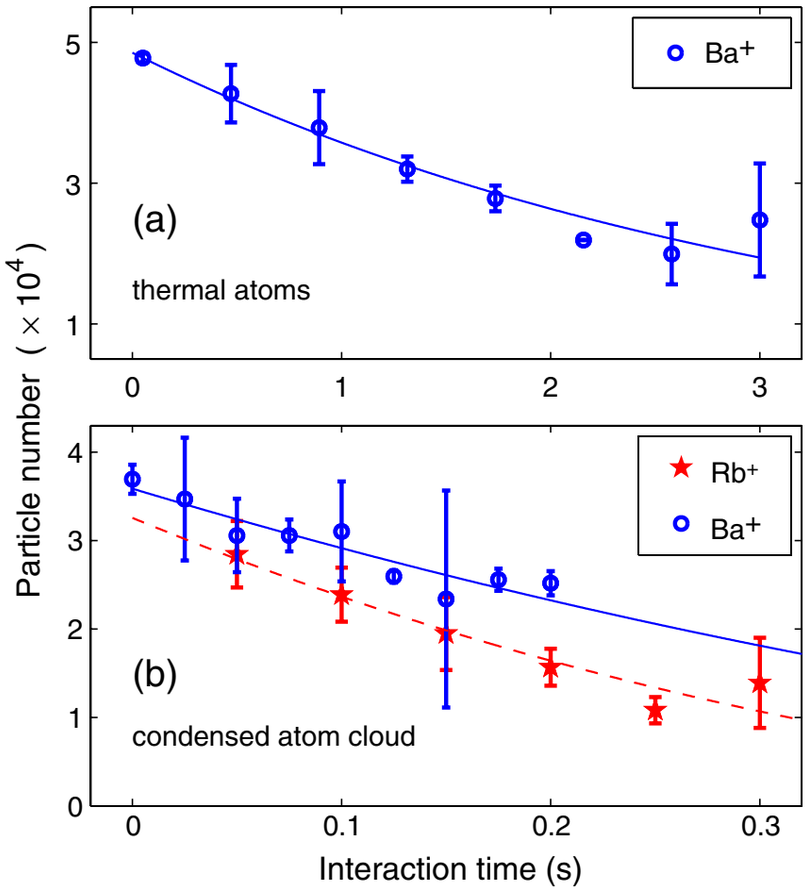

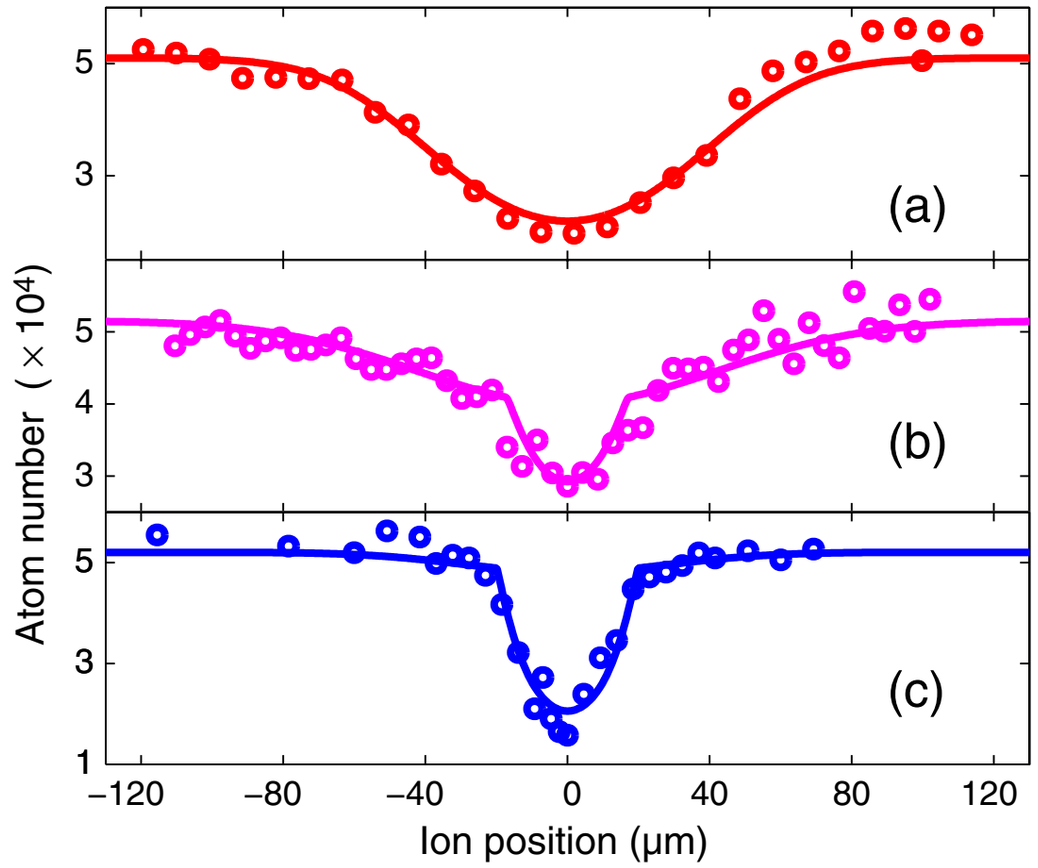

thermal atom cloud

partially condensed atom cloud

Bose-Einstein condensate

S. Schmid et al., PRL 105 (2010), 133202

- Minimizing the atom loss rate as a function of the position of the ion in the trap can be used to minimize the ion micromotion.

A. Härter et al., Appl. Phys. Lett. 102 (2013), 221115

Sympathetic cooling of ions by atoms

- Elastic collisions with ultracold atoms lead to the sympathetic cooling of the trapped ions.
- Ultracold atoms are heated by the collisions and are lost from the trap.

Sympathetic cooling of a single Yb^+ ion with ultracold Rb atoms

C. Zipkes et al., Nature 464 (2010), 388

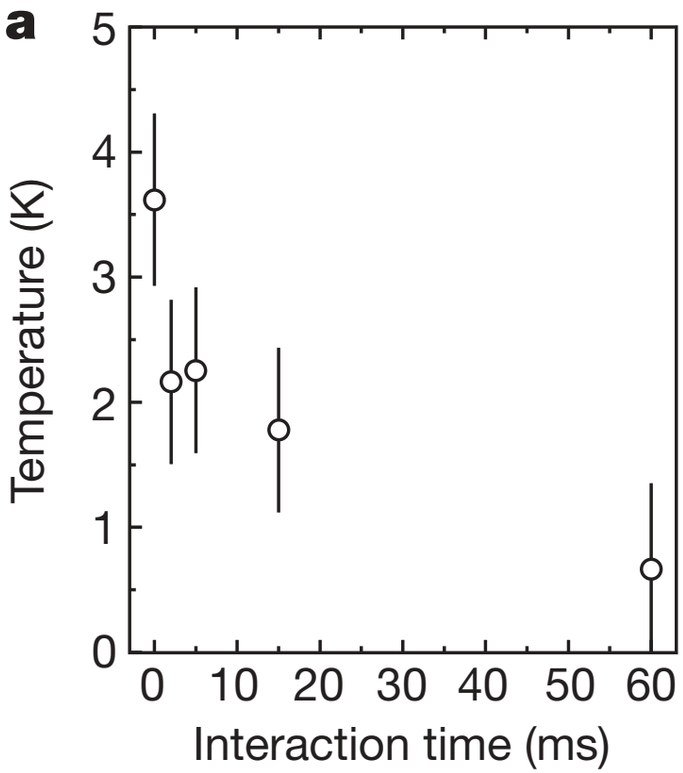

Yb^+ ion temperature as a function of the interaction time with ultracold Rb atoms

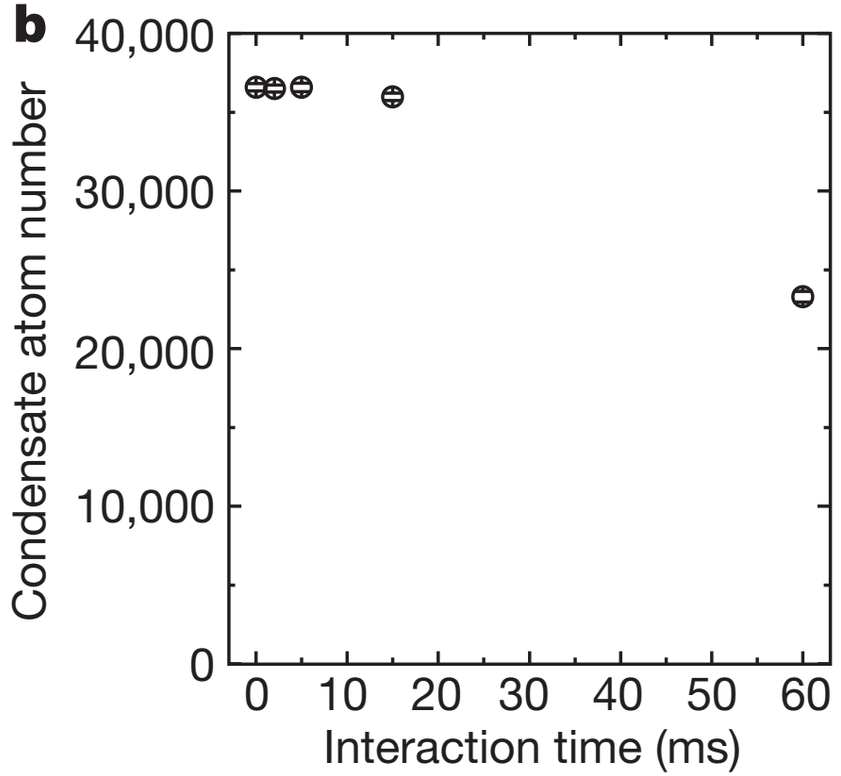

Ultracold atom number as a function of the interaction time with a single Yb^+ ion

Cold reactive ion-atom collisions

Light-assisted processes

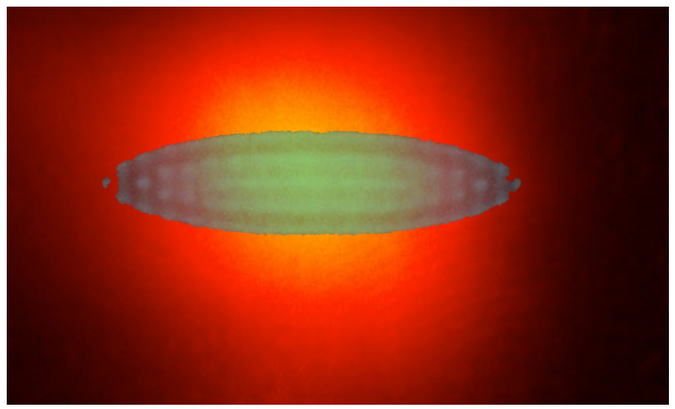

A Ca^+ Coulomb crystal immersed in a cloud of ultracold Rb atoms

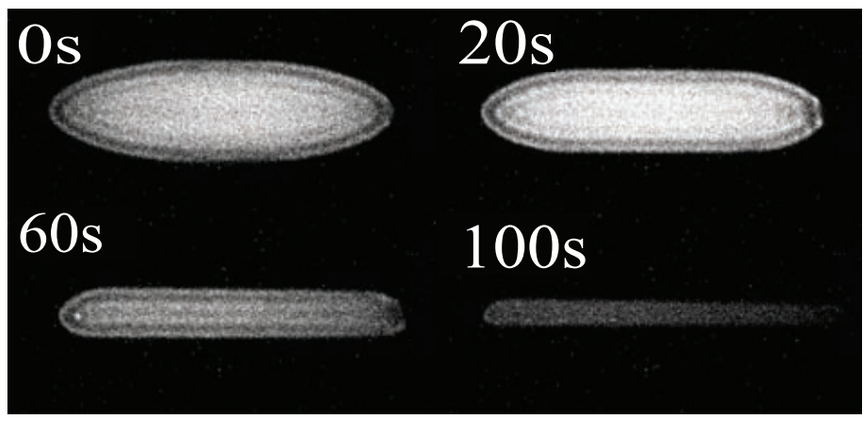

Removal of Ca^+ ions because of chemical reactions between Ca^+ and Rb (only Ca^+ fluorescence shown)

- **Resonant-excitation mass spectra of reaction products:**

  3 reaction products: Rb^+, $CaRb^+$ and Rb_2^+

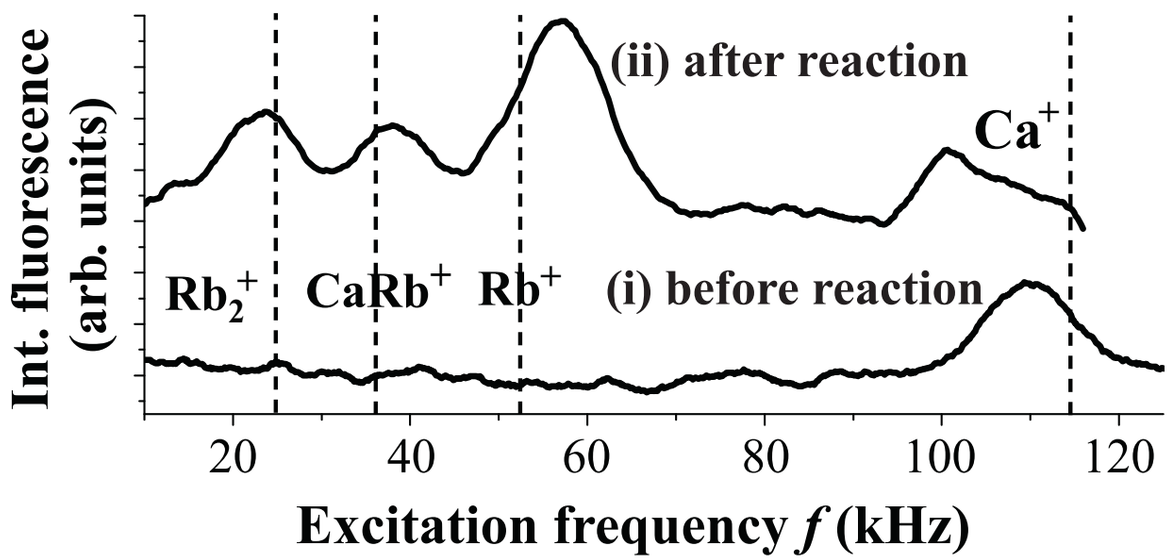

F.H.J. Hall, M. Aymar, N. Bouloufa, O. Dulieu and SW, Phys. Rev. Lett. 107 (2011), 243202
F.H.J. Hall, P. Eberle, G. Hegi, M. Aymar, M. Raoult, O. Dulieu, SW, Mol. Phys. 111 (2013), 2020
F.H.J. Hall,M. Aymar, M. Raoult, O. Dulieu and SW, Mol. Phys. 111 (2013), 1683

Potential-energy curves of $CaRb^+$: reaction mechanisms

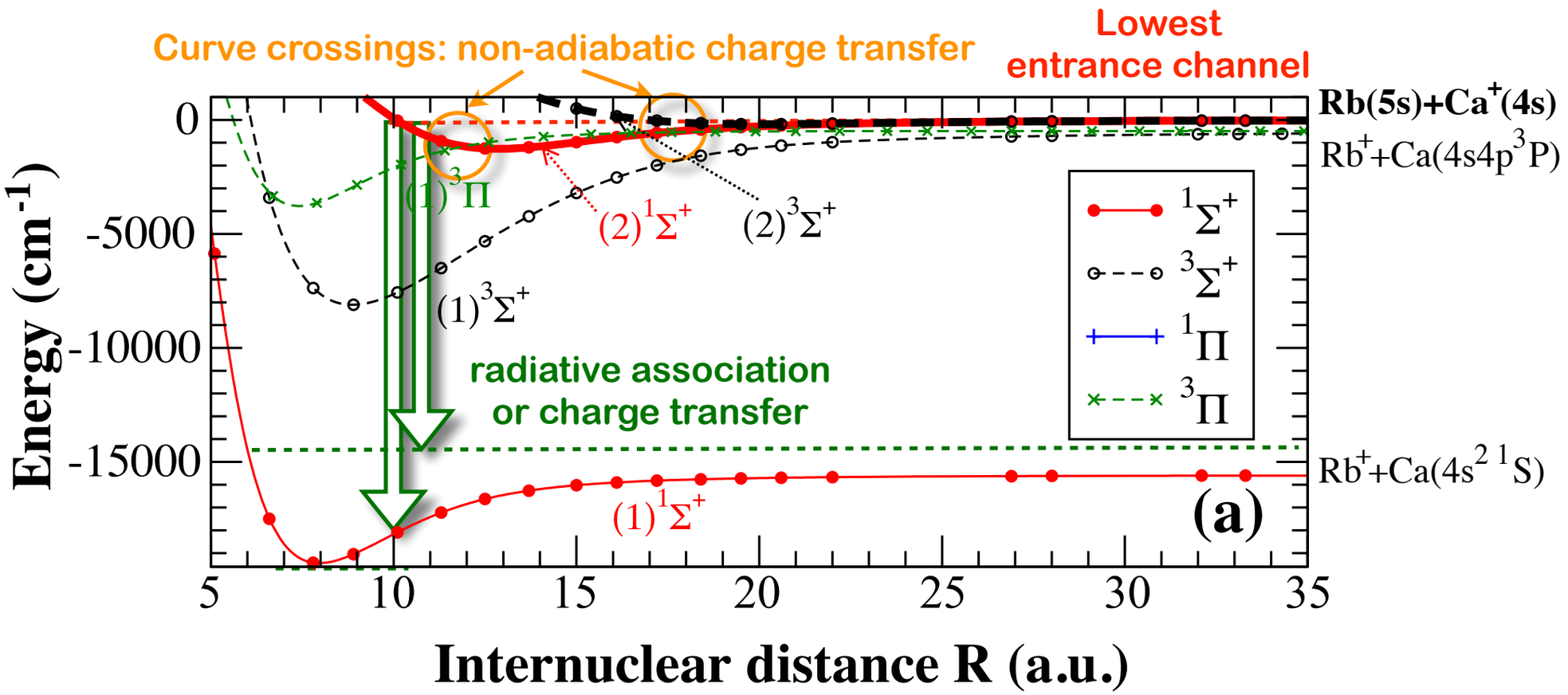

3 reactive processes:

- non-radiative charge transfer by non-adiabatic transitions at crossings between two potential-energy curves
- radiative charge transfer by emission of a photon to a lower-lying scattering state
- radiative association of a molecular ion by emission of a photon to a lower-lying bound molecular state

State dependence of reaction rates

- **Measured rate constants as a function of Ca^+ level populations:**

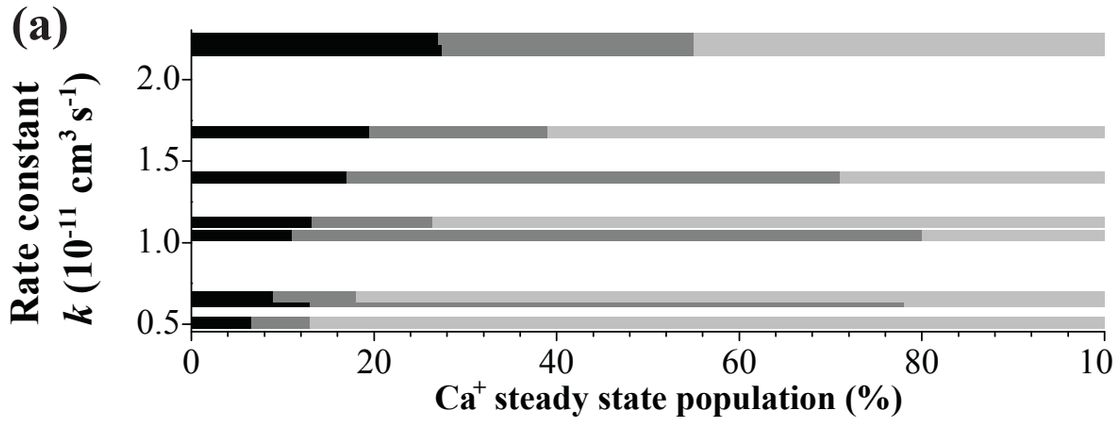

Rate constants:

$^2S_{1/2}$: $k_s = 3 \cdot 10^{-12}$ cm^3 s^{-1}

$^2P_{1/2}$: $k_p = 1.5(6) \cdot 10^{-10}$ cm^3 s^{-1}

$^2D_{3/2}$: $k_d < 3 \cdot 10^{-12}$ cm^3 s^{-1}

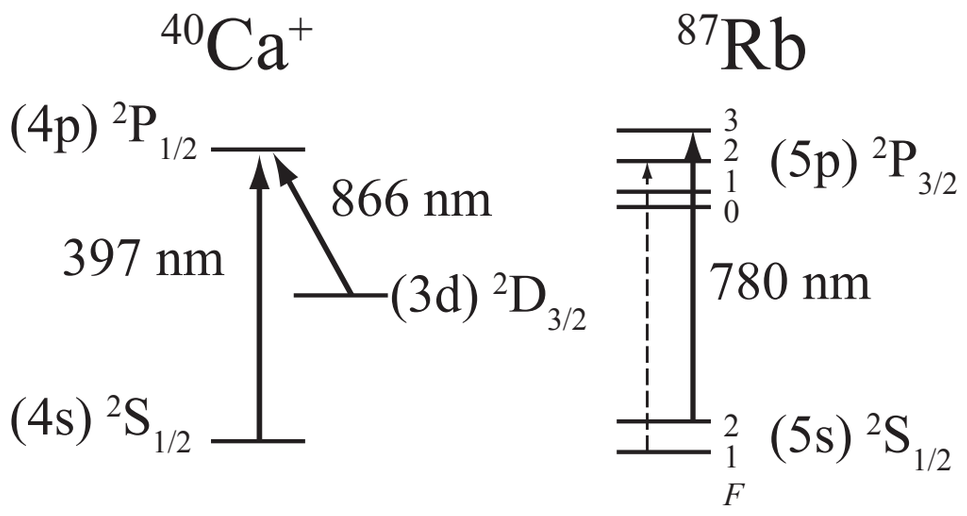

- **Potential energy curves of excited states:**

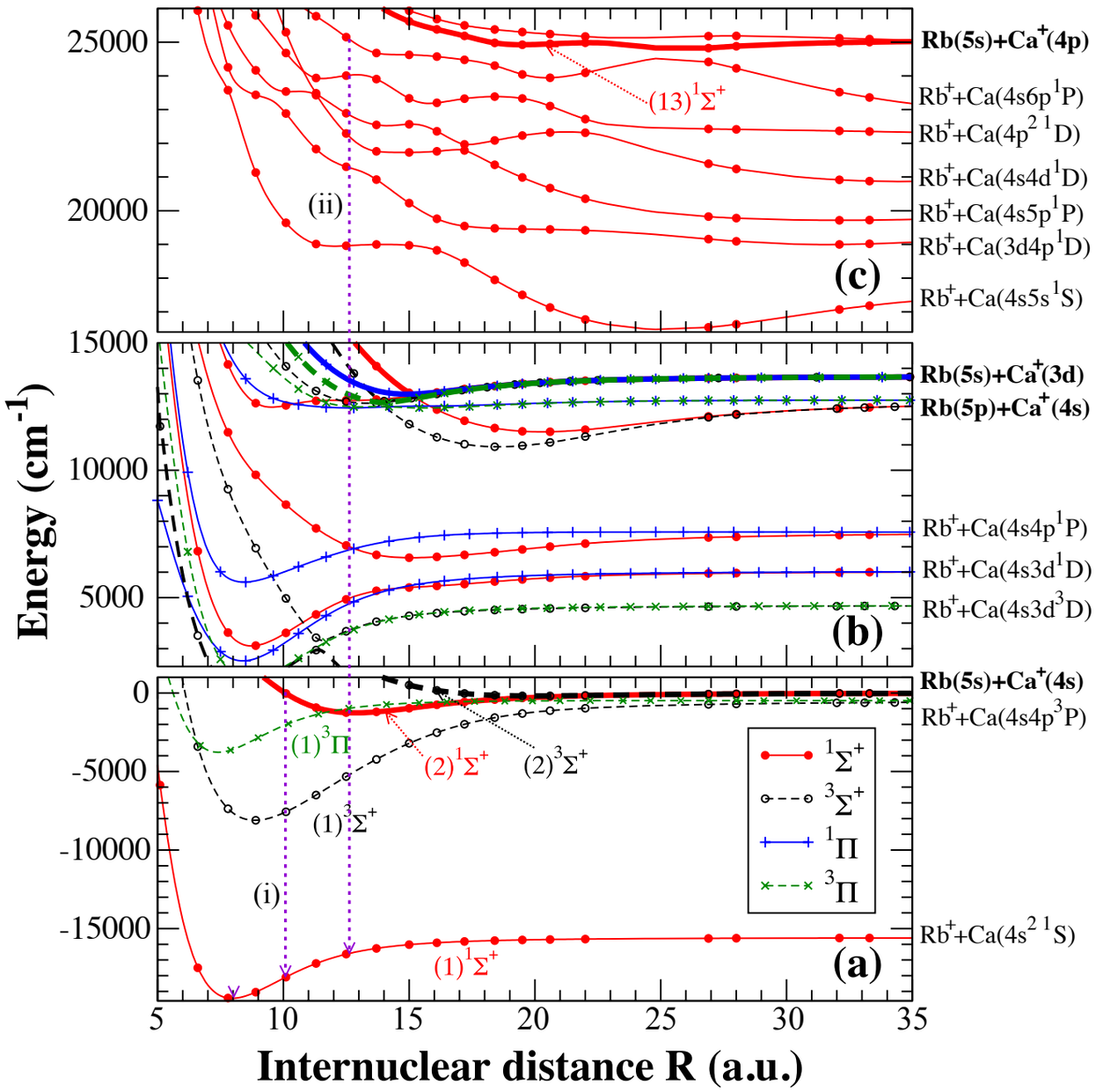

"Universal" cold reaction dynamics:

- **Energy-dependence of rate constants for cold reactions:**

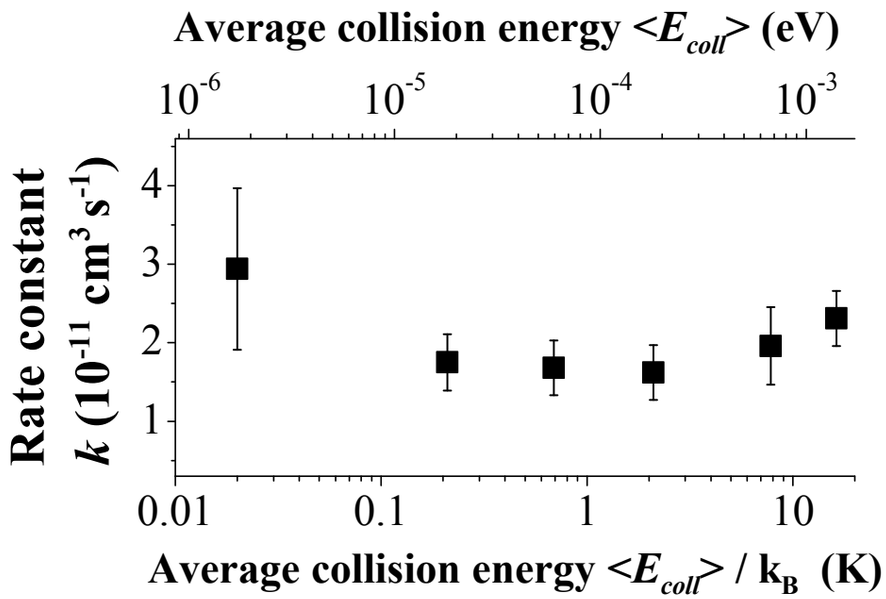

$Ca^+ + Rb$

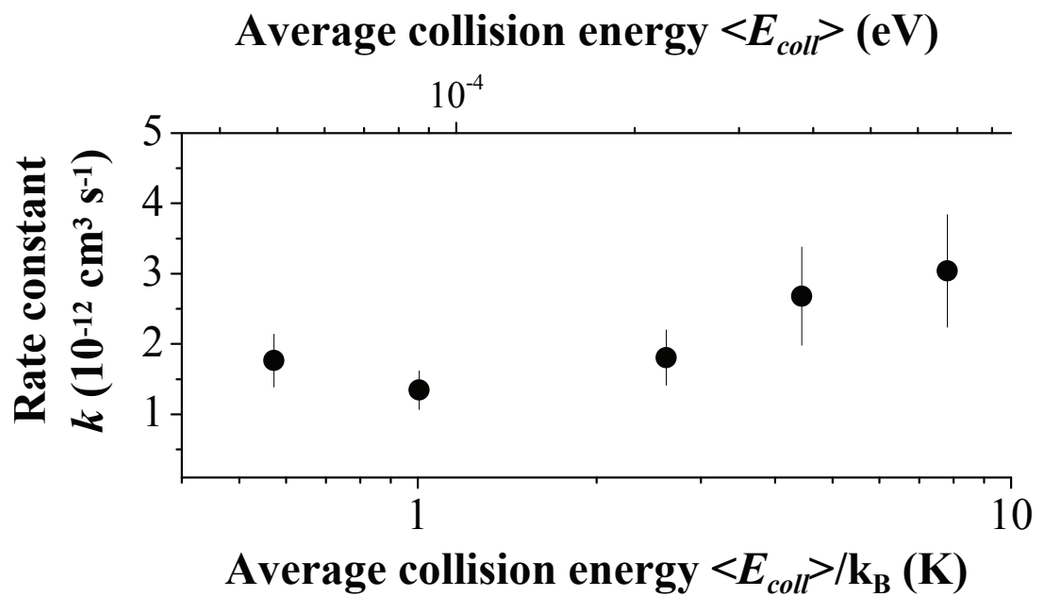

$Ba^+ + Rb$

The rate constant does not (or only weakly) scales with the energy for all cases, in line with classical Langevin theory !

F.H.J. Hall, et al., Mol. Phys. 111 (2013), 2020

Quantum theory for radiative association and charge transfer: cross sections

- **Radiative charge transfer:**

$$\sigma^{RCT}(\epsilon_i) = p \quad \frac{8\pi^2}{3c^3}\frac{1}{k_i^2}\sum_{J=0}^{\infty}\int_0^{\epsilon_f^{max}} \omega_{i,f}^3 \left(J|\langle J-1,\epsilon_f|D(R)|\epsilon_i,J\rangle|^2 + (J+1)|\langle J+1,\epsilon_f|D(R)|\epsilon_i,J\rangle|^2\right) d\epsilon_f$$

collision energy of reactants — transition dipole moments (TDMs) — kinetic energy of products

- **Radiative association:**

$$\sigma^{RA}(\epsilon_i) = p\,\frac{8\pi^2}{3c^3}\frac{1}{k_i^2}\sum_{J=0}^{\infty}\sum_{v=0}^{v_{max}}\left(\omega_{iJ,v(J-1)}^3 J|\langle J-1,v|D(R)|\epsilon_i,J\rangle|^2 + \omega_{iJ,v(J+1)}^3 (J+1)|\langle J+1,v|D(R)|\epsilon_i,J\rangle|^2\right).$$

B. Zygelman, A. Dalgarno, PRA 38 (1988), 1877

- **Non-radiative charge transfer:**

$$\sigma^{NRCT} = \frac{\pi\hbar^2 p}{2\mu E}\sum_{J=0}^{\infty} P_{if}(J,E)(2J+1)$$

M. Tacconi et al., PCCP 13(2011), 19156

where p is the statistical weight of the initial scattering state and P_{if} is the non-adiabatic transition probability between the initial and the final scattering state. If the non-adiabatic transition is effected by spin-orbit (SO) coupling (as in Ca^+ + Rb), then P_{if} can be formulated as: $P_{if}(J,E) = \left|2\mu\int_0^{\infty}\langle\Psi_f|H_{so}|\Psi_i\rangle dR\right|^2$ **with H_{so} ... SO coupling operator**

Transition to universal classical dynamics:

- Couplings localized in deep potential well: TDMs independent of collision energy ε_i
- TDMs independent of J for large J: factor TDMs out of sum over J
- Thus: $\sigma \propto J_{\max}^2/k_i^2 \equiv b_{\max}^2$ as predicted by classical collision theory
- For $b_{\max} \propto \epsilon_i^{-1/4} \Rightarrow k = \text{const.}$

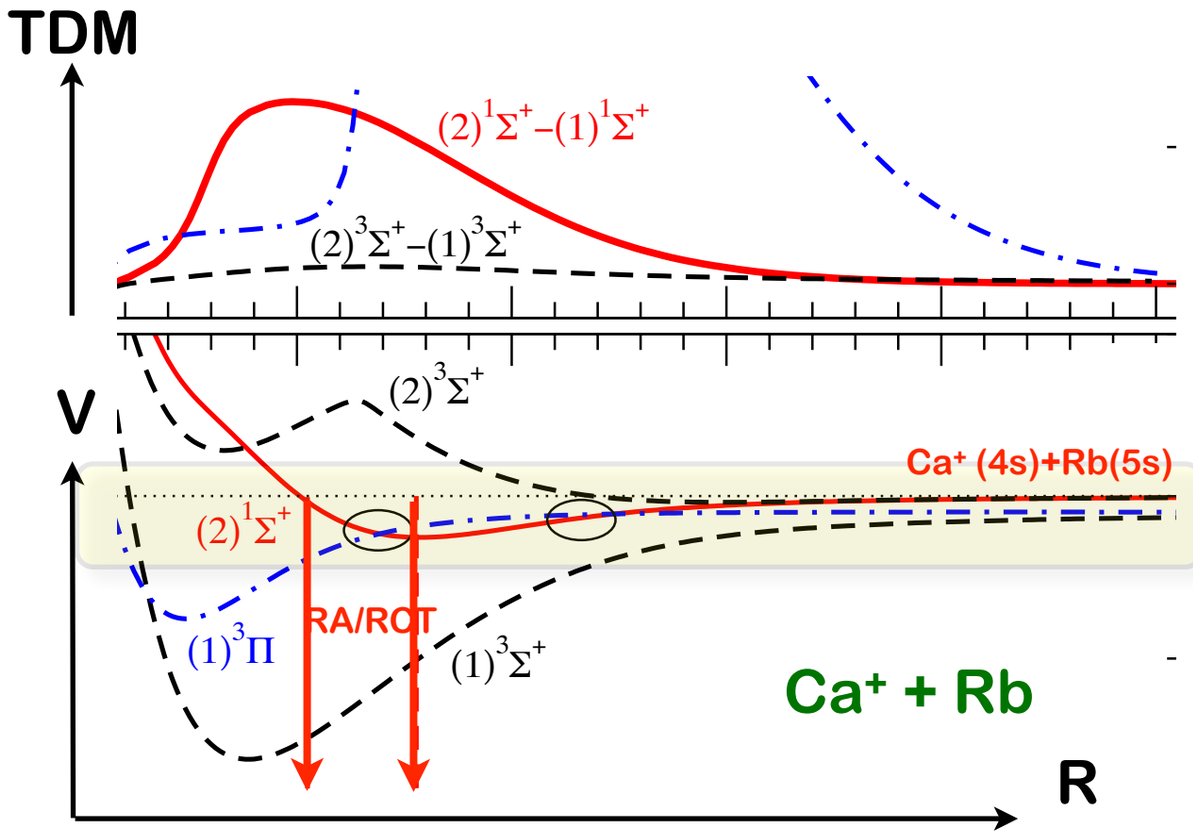

Thus, the energy dependence of the rate constants can be explained in terms of a classical collision model in line with Langevin theory. The absolute magnitude of the rate constants, however, is determined by the strength of the short-range non-adiabatic and radiative couplings.

Engineering excited-state interactions

- Collisions with atoms in excited states, e.g., populated by excitation during laser cooling, are suppressed when the time for collision is comparable or longer than the lifetime of the excited state, e.g., in the Ca - Yb^+ system. In this case, the excited state of the atom decays before reactive processes such as charge exchange can occur at short range.

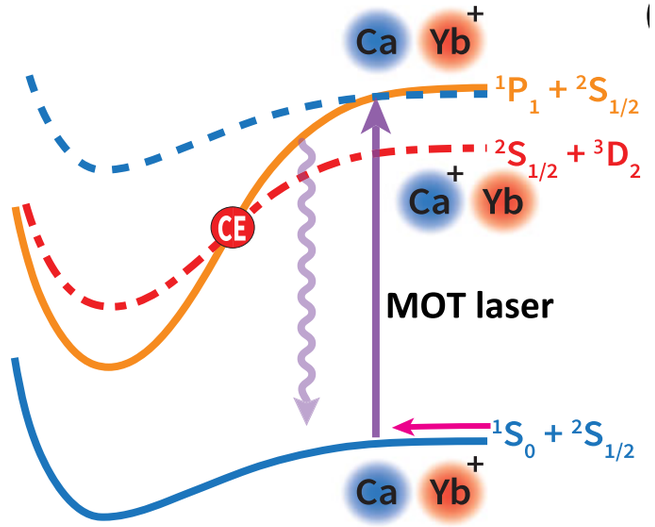

Charge exchange (CE) in the excited $^1P_1$ state of Ca with Yb^+ is suppressed by spontaneous emission during the collision before the system can reach the CE region at short distances.

- A "catalyst laser" laser can be introduced to excite the system right during the collision at short range thus promoting charge exchange in the excited channel.

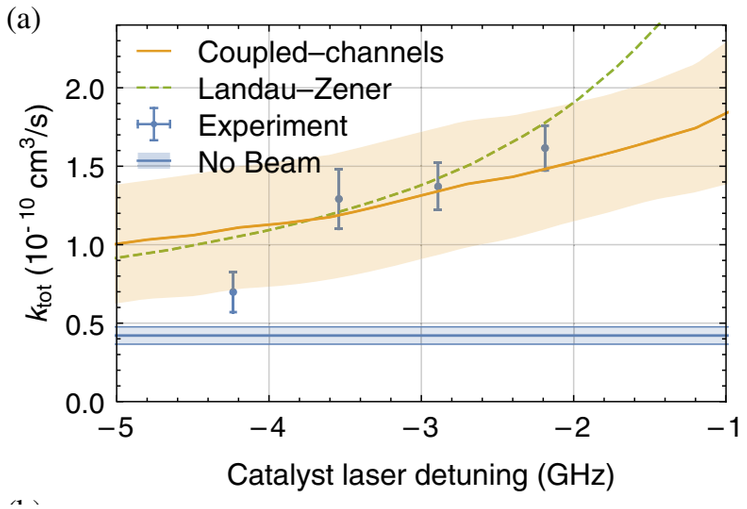

Promotion of charge exchange by a catalyst laser: Charge-exchange rate constant for Ca-Yb^+ as a function of the detuning of the catalyst laser from the $^1S_0$-$^1P_1$ transition in Ca.

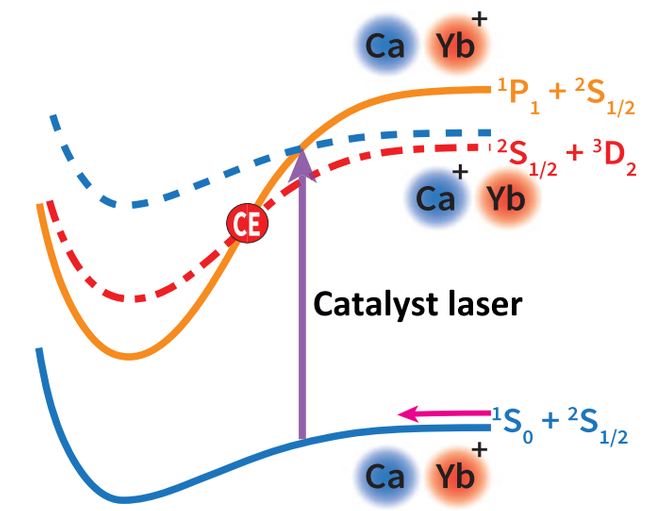

The introduction of a "catalyst laser" at a suitable wavelength excites the system during the collision promoting charge exchange.

M. Mills et al., PRL 122 (2019), 233401

Cooling of trapped ions by charge exchange ("swap" cooling)

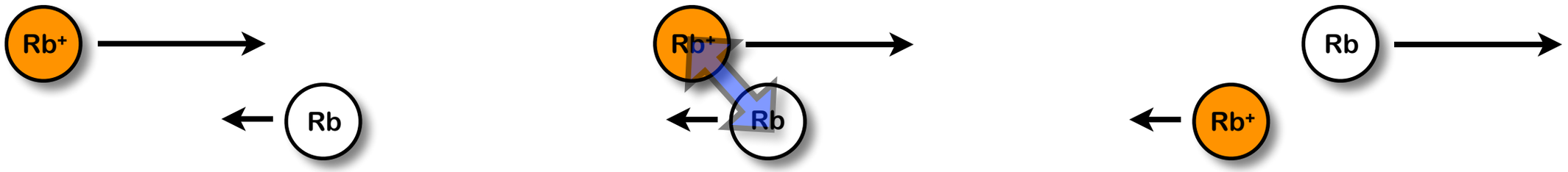

fast ion, slow atom | charge exchange | slow ion, fast atom

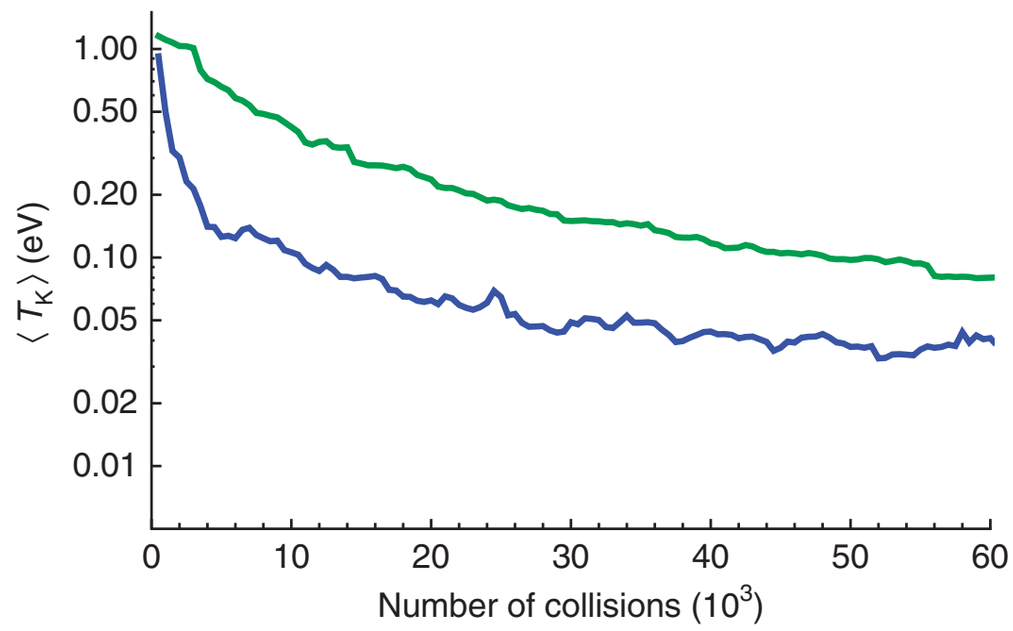

Simulated ion temperature with and without charge-exchange cooling

K. Ravi et al., Nature Commun. 3 (2012), 1126

Experimental demonstration: A. Mahdian et al., arXiv 2012.07759

Three-body recombination processes between two ultracold atoms colliding with an ion

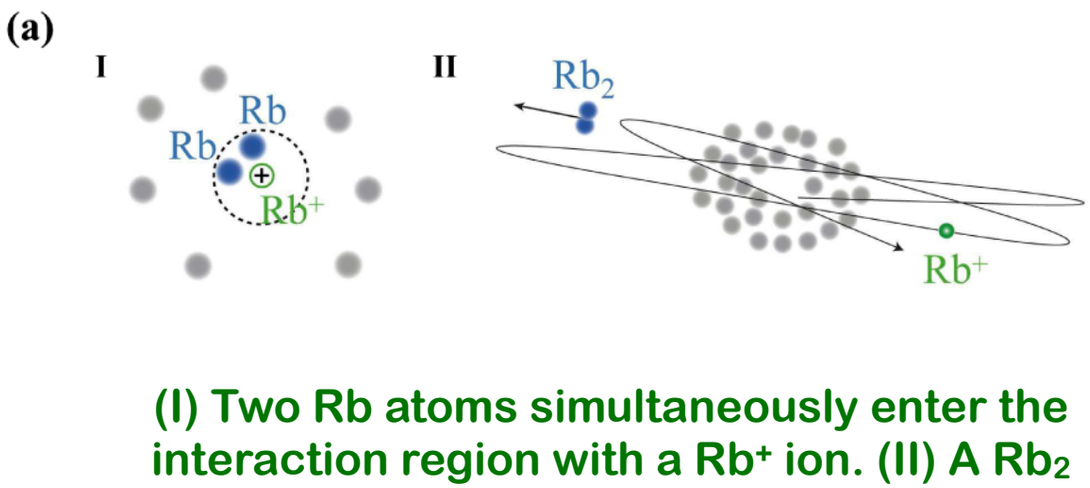

(I) Two Rb atoms simultaneously enter the interaction region with a Rb^+ ion. (II) A Rb_2 molecule is formed in a three-body collision. The energy released in the process sends the Rb^+ on a large trajectory in the trap.

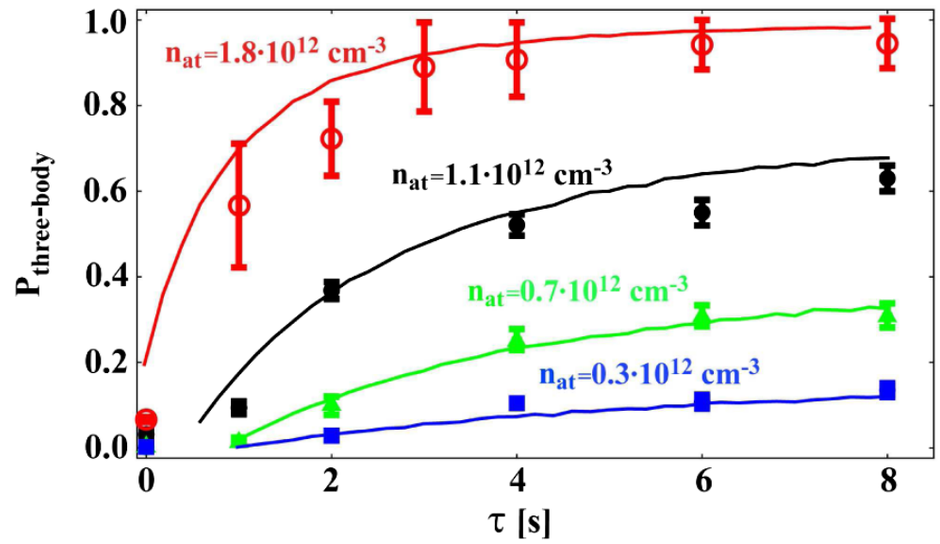

Probability for a three-body recombination process as a function of the interaction time for different atom densities n_{at}

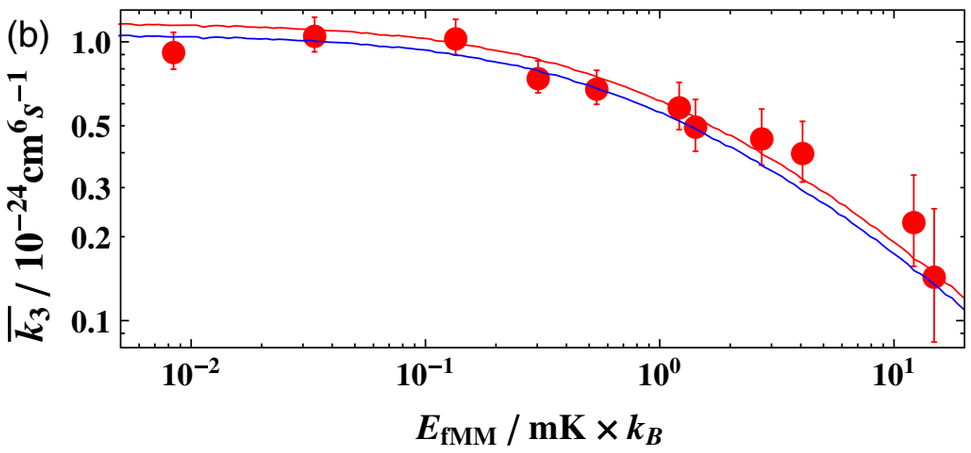

Three-body rate coefficient as a function of the ion energy for $Ba^+ + Rb + Rb \rightarrow BaRb^+ + Rb$

A. Härter et al., PRL 109 (2012), 123201
A. Krükow et al., PRL 116 (2016), 193201

Limits to sympathetic cooling: Micromotion heating of ions by (ultracold) buffer gases

Micromotion-Induced Limit to Atom-Ion Sympathetic Cooling in Paul Traps

M. Cetina et al., PRL 109 (2012), 253201

- Due to the time-varying fields in RF ion traps, the ions undergo a fast oscillating motion driven by the RF fields ("micromotion") in addition to a slow thermal ("secular") motion (see chapter 1)
- The micromotion vanishes in the centre of the trap where the RF fields are zero, but does not vanish elsewhere
- It usually represents the dominant contribution to the ion kinetic energy

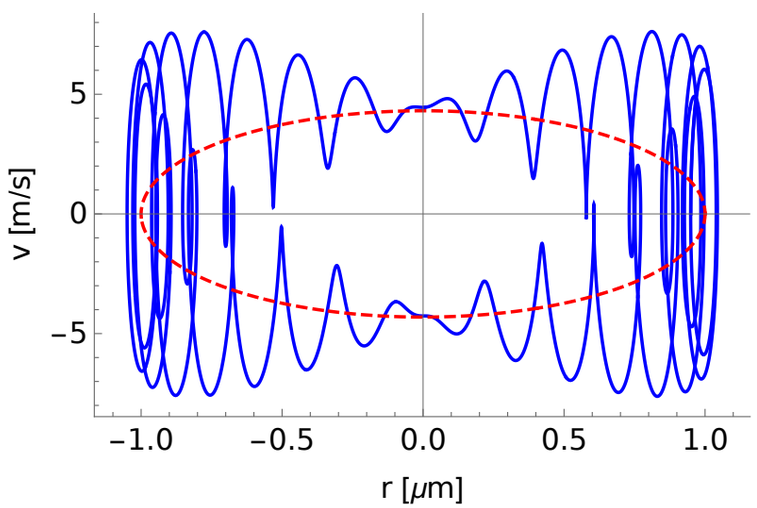

1D phase-space trajectory of an ion with (blue) and without (red) micromotion

I. Rouse and SW, Mol. Phys. 117 (2019), 3120

- Even if the ions are perfectly aligned with the RF null line in the centre of a linear Paul trap, they are pulled away by attractive interactions during the collision with a neutral particle
- The RF field can does perform work on the ion during a collision, ultimately leading to heating and setting limits to the collision energy

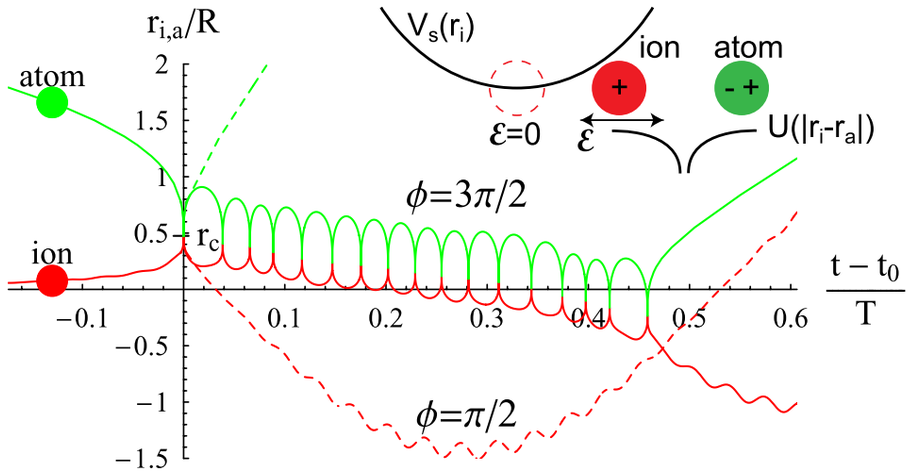

Examples of trajectories of an ion and an atom during a classical 1D low-energy collision at different phases φ of the RF field.

φ=π/2: collision leads to heating of ion

φ=3π/2: initial removal of energy from the ion, but frequent recollisions lead to eventual heating

M. Cetina et al., PRL 109 (2012), 253201

- The heating induced by the micromotion depends on the mass ratio of the neutral and the ion. Cold buffer gases which are too heavy do not, in fact, lead to cooling, but to heating of the ions. F. G. Major and H. G. Dehmelt, Phys. Rev. 170, 91 (1968)

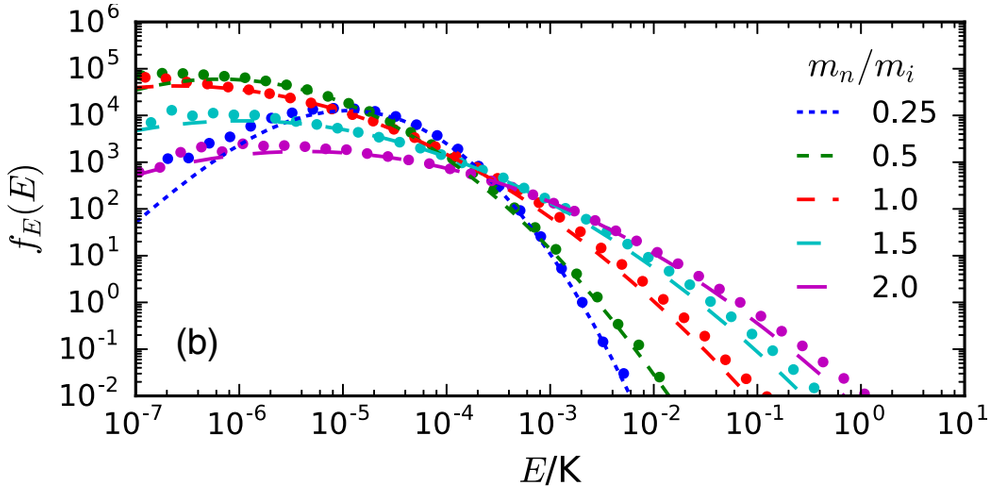

Simulated energy distributions of a cold ion in an RF trap after 25 ion-neutral collisions for different neutral-ion mass rations m_n/m_i for a buffer gas held at T=0 K. The micromotion heating becomes more pronounced with increasing m_n/m_i, i.e., heavier buffer gases.

I. Rouse and SW, PRL 118 (2017), 143401

- This effect can be mitigated by a localisation of the buffer gas, i.e., for cases in which the ion trajectory is larger than the extent of the buffer gas

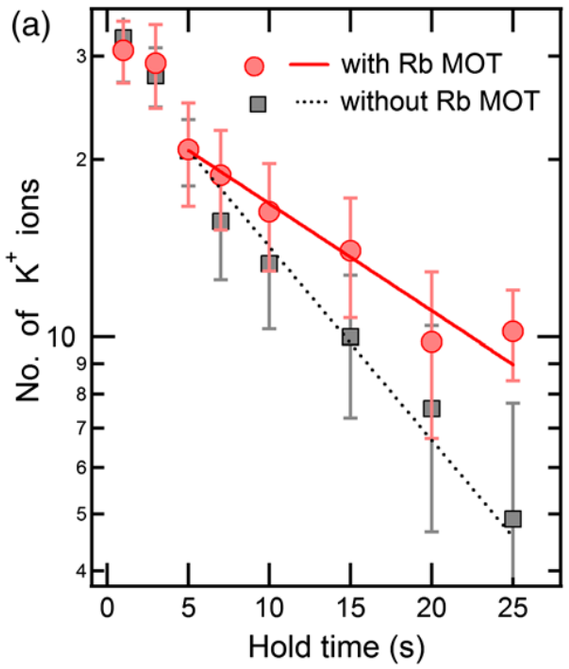

Number of $^{39}K^+$ ions remaining in an ion trap as a function of the hold time with and without a localised buffer gas of ultracold ^{85}Rb atoms held in a MOT. The localisation of the buffer gas leads to a partial cooling of the initially hot ions (prolonging their trap lifetime) in spite of the adverse neutral-ion mass ratio.

S. Dutta et al., PRL 118 (2017), 113401

Further reading:

- R.G. DeVoe, PRL 102 (2009), 063001
- C. Zipkes et al., NJP 13 (2011), 053020
- K. Chen et al., PRL 112 (2014), 143009
- B. Höltkemeier et al., PRL 116 (2016), 233003
- I. Rouse et al., PRA 97 (2018), 042712
- I. Rouse et al., Mol. Phys. 117 (2019), 3120

Experimental demonstration of micromotion heating in hybrid traps: Dynamics of a ground-state cooled ion colliding with ultracold atoms

Z. Meir, T. Sikorsky, R. Ben-shlomi, N. Akerman, Y. Dallal, and R. Ozeri, PRL 117 (2016), 243401

- Interactions of ultracold Rb atoms (T≈5 μK) with Sr^+ ions cooled to the motional ground state of the trap:

a

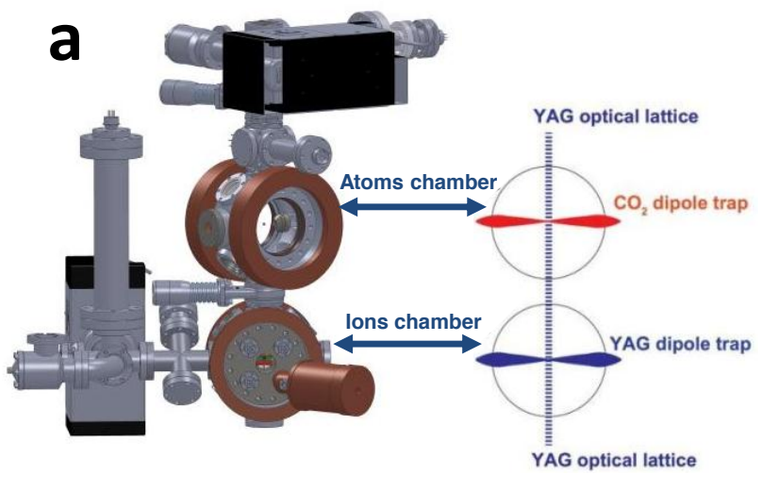

c

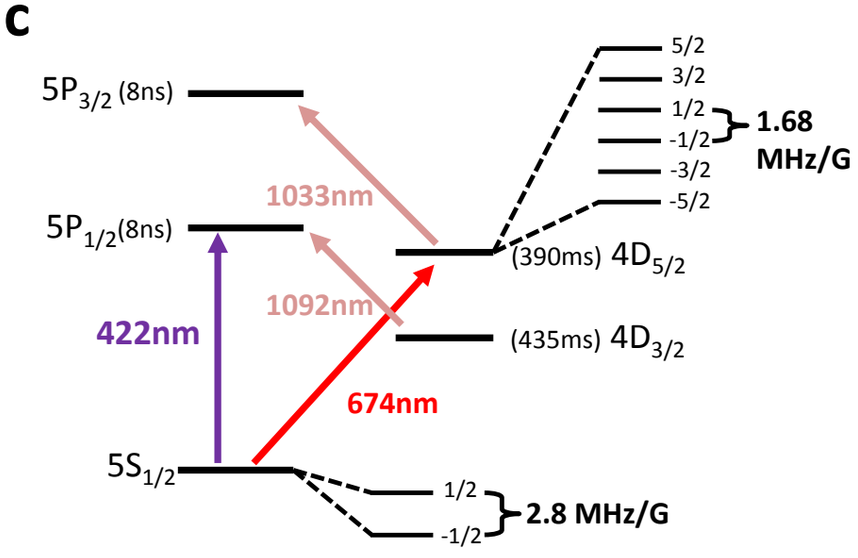

- The cold ions collide with the ultracold atoms in the RF field of the ion trap. The resulting coupling of micromotion with the secular motion leads to ion heating and a non-thermal distribution of the ion energies E which is often modelled by a Tsallis distribution:

$$P(E) = \frac{(n-3)(n-2)(n-1)}{2(nk_B T)^3} \frac{E^2}{\left(1+\frac{E}{nk_B T}\right)^n}$$

with $n = \frac{1}{q_T - 1}$

q_T is the Tsallis parameter which describes the deviation from thermal (Boltzmann) behaviour. For $q_T \to 1$, P(E) becomes a thermal distribution.

see also: I. Rouse and SW, PRL 118 (2017), 143401

Cold molecular ions in traps: methods and applications

- **Rabi flops as a function of collision time in the interval t=0-6.5 ms (a-f) with ultracold Rb atoms and fits assuming thermal vs. Tsallis statistics:**

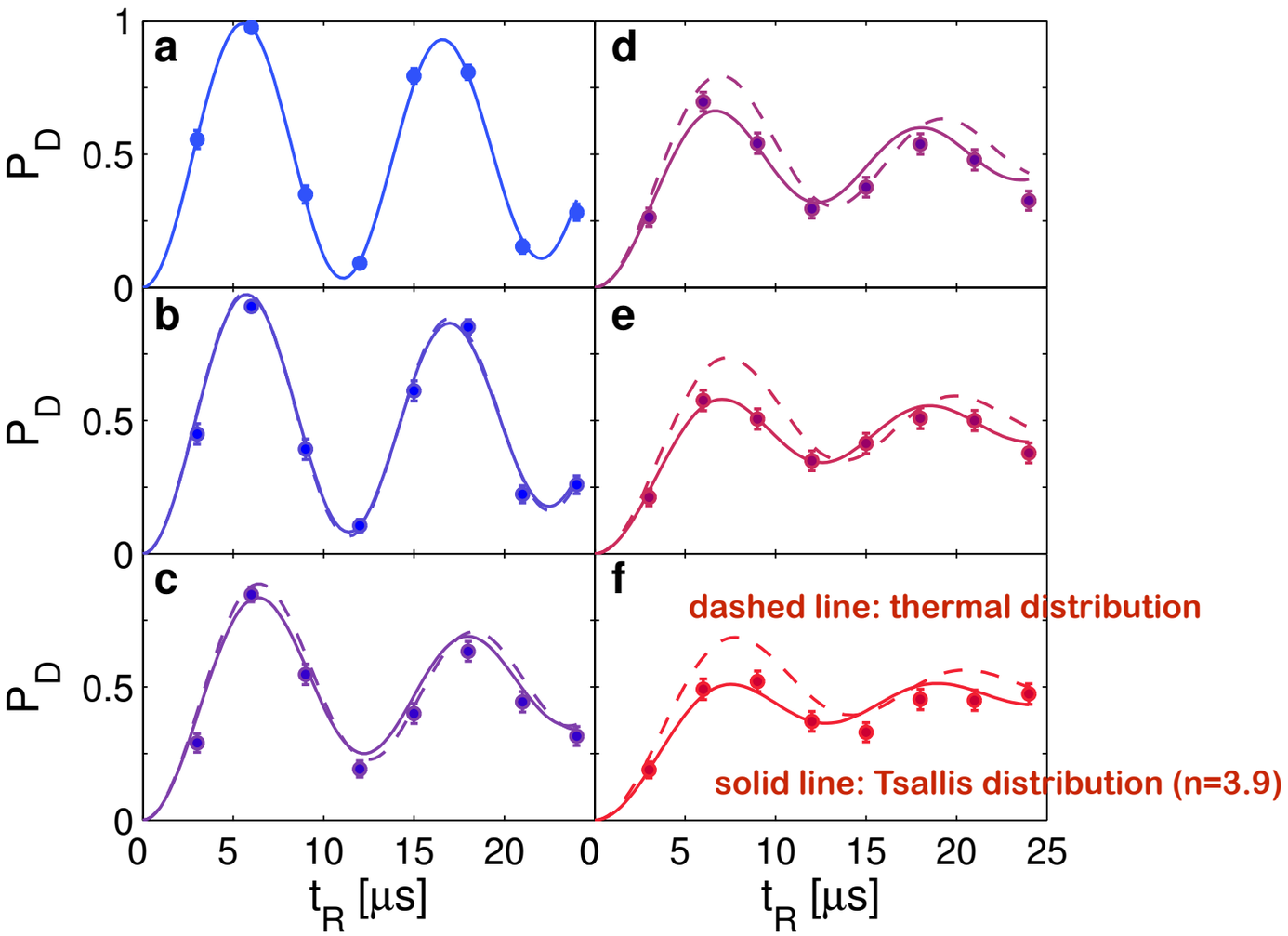

- **Ion temperature and n-exponent as a function of the number of collisions with the atoms:**

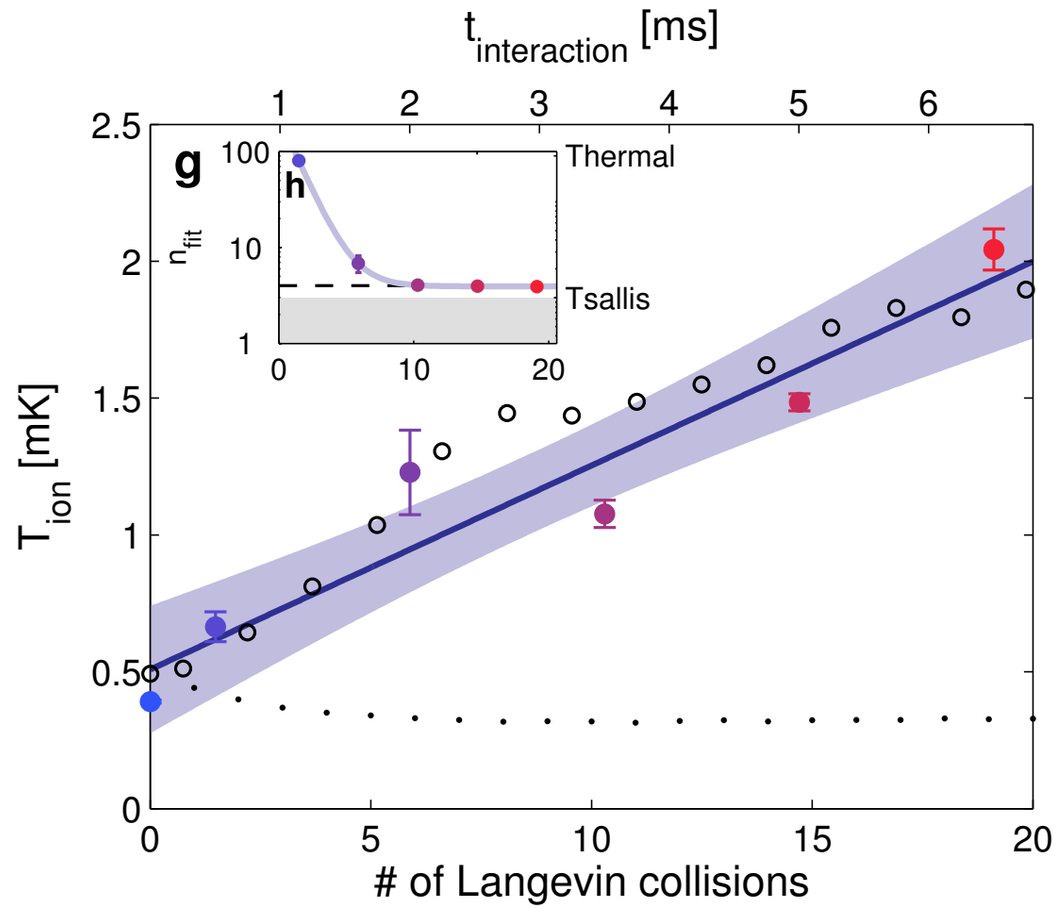

Cold molecular ions in traps: methods and applications

- **Ion heating dynamics and steady-state temperature**

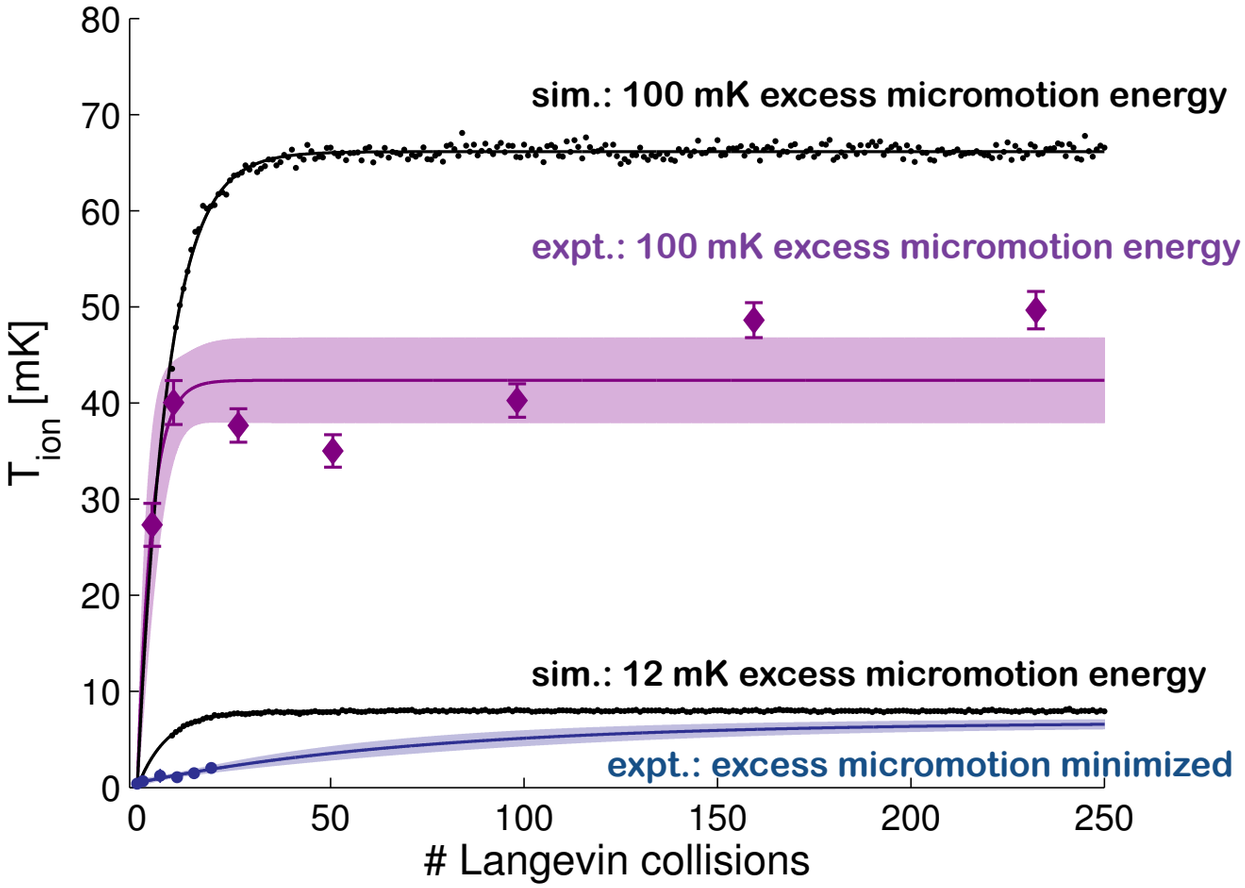

- **Despite initially being cooled to the motional ground state, the steady-state temperature was determined to be T≈7 mK.**

- **Conclusions: despite the initial ultracold temperatures of both ions and atoms, the ion heating dynamics through collisions in the RF field leads to ca. 3 order of magnitude higher steady state temperatures. In this case, ultracold (T<1 mK) processes can only be studied during the first few collisions.**

Ultracold ion-atom collisions

- Because of its dependence on the neutral-ion mass ration, the problems with micromotion heating of the ions can be mitigated by pairing a light buffer gas with heavy ions.
- Choosing a very light ultracold buffer gas (^{6}Li) with a very heavy ion (^{171}Yb$^+$) recently enabled the observation of quantum signatures in ultracold ion-atom collisions in the few-partial-wave regime

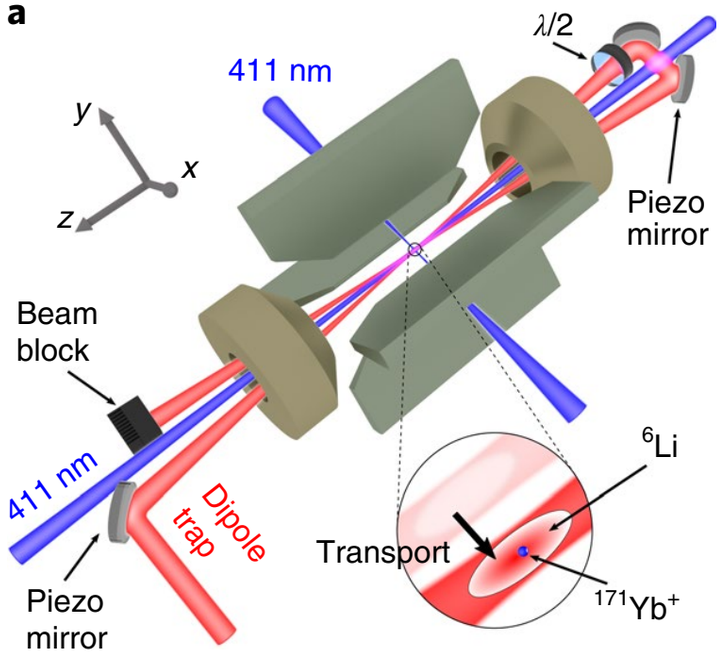

Experiment: Yb$^+$ ions in a RF trap immersed into ultracold Li atoms in an optical dipole trap

T. Feldker et al., Nat. Phys. 16 (2020), 413

- After Doppler laser cooling, the Yb$^+$ are buffer-gas cooled by the ultracold Li atoms (at T=2 μK) to T≈100 μK limited by residual micromotion heating.
- Note that because of the kinematics of the collisions with reduced mass μ, the collision energy between ions (energy E_i) and atoms (Energy E_a) is given by:

$$E_{\mathrm{col}} = \frac{\mu}{m_i} E_i + \frac{\mu}{m_a} E_a$$

yielding $E_{\mathrm{col}} \lessapprox 10$ μK which is much smaller than the ion energy and close to the s-wave regime.

- Subsequently, spin-exchange collisions for Yb^+ ($F=1 \rightarrow F=0$) with Li were studied as a function of the collision energy
- The collision energy was tuned by imparting the ions excess micromotion by moving them away from the trap axis with static electric fields

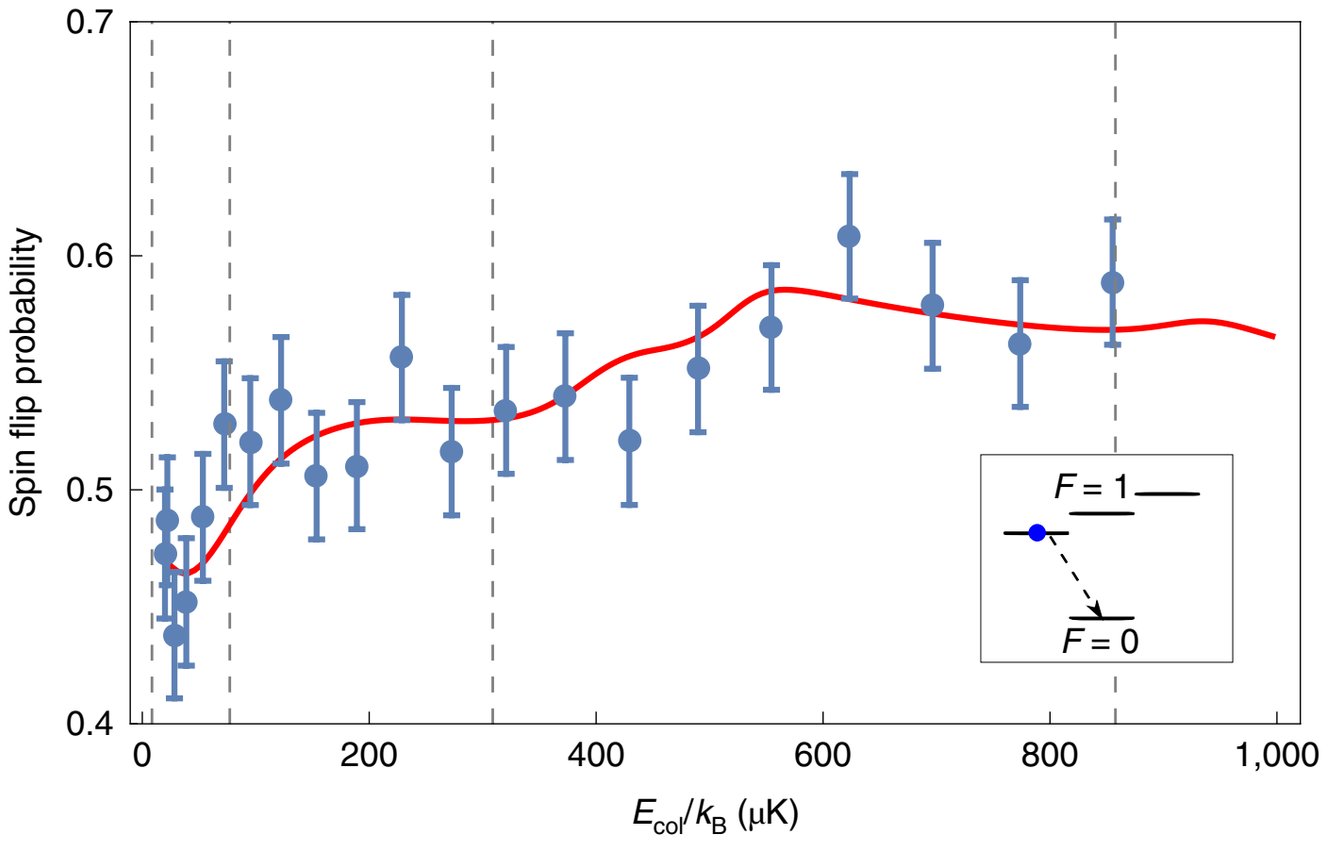

- The collision cross section was found not to be constant with E_{col}, as predicted by Langevin theory, but showed a clear energy dependence and structure.
- Using quantum scattering calculations (red line in the figure), the data could be interpreted in terms of quantum signatures in the collisions such as shape resonances.

7. Molecular ions in hybrid traps

Charge transfer dynamics in N_2^+ / O_2^+ + Rb

- Molecular ions are produced by photoionization and sympathetically cooled into a Ca^+ Coulomb crystal
- Charge exchange according to:
  $N_2^+ / O_2^+ + Rb \rightarrow N_2 / O_2 + Rb^+$
- Reactions in Rb (5s) $^2S_{1/2}$ and (5p) $^2P_{3/2}$ states

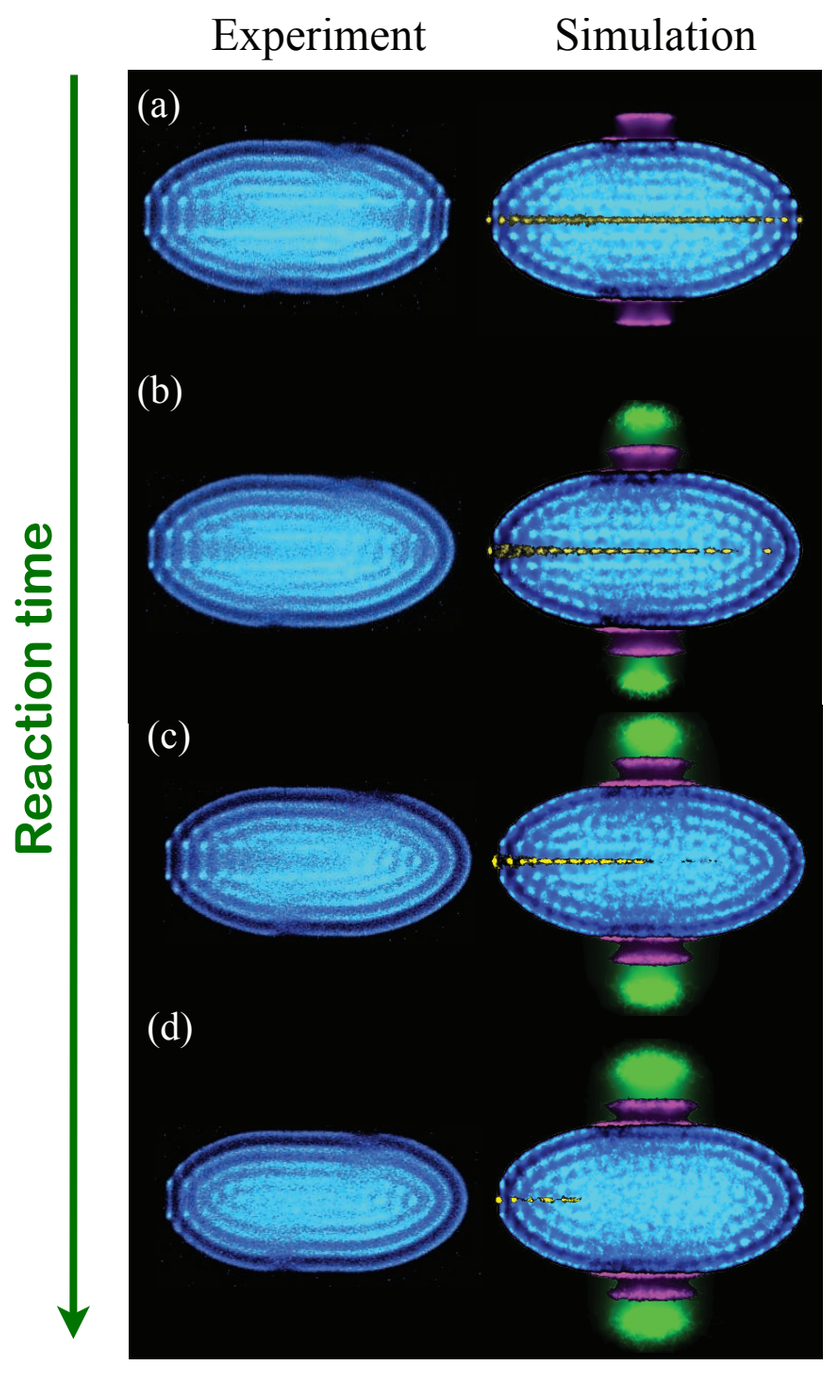

F.H.J. Hall and SW, Phys. Rev. Lett. 109 (2012), 233202

Tuning collision energies: a "dynamic" ion-atom hybrid trap for cold atoms and molecular ions

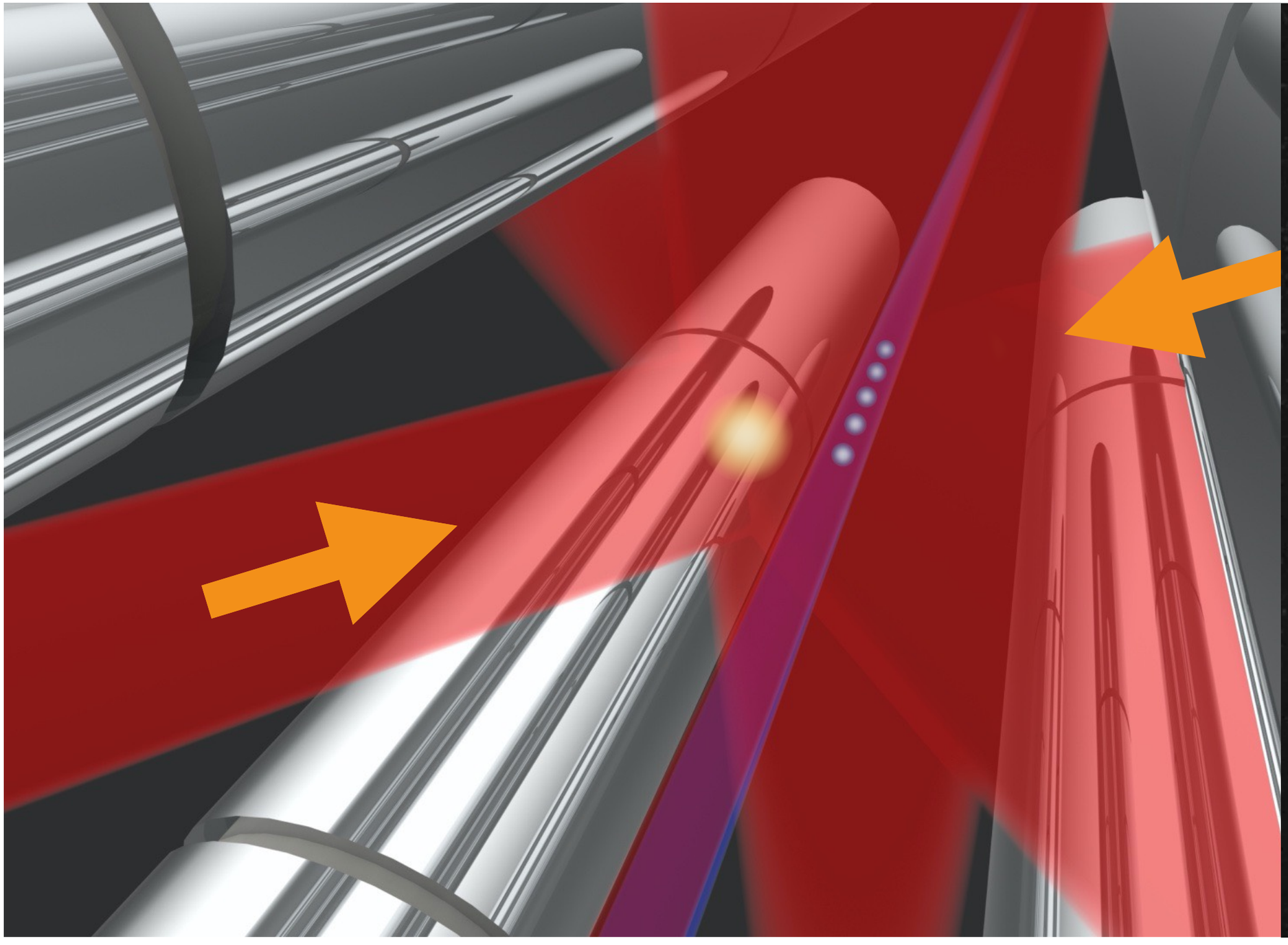

P. Eberle, A. D. Dörfler, C. von Planta, K. Ravi and SW, ChemPhysChem, 17 (2016), 3769

Electron transfer in the millikelvin regime:

$N_2^+ + Rb \rightarrow N_2 + Rb^+$

$O_2^+ + Rb \rightarrow O_2 + Rb^+$

- **Entrance and product channels for electron transfer**

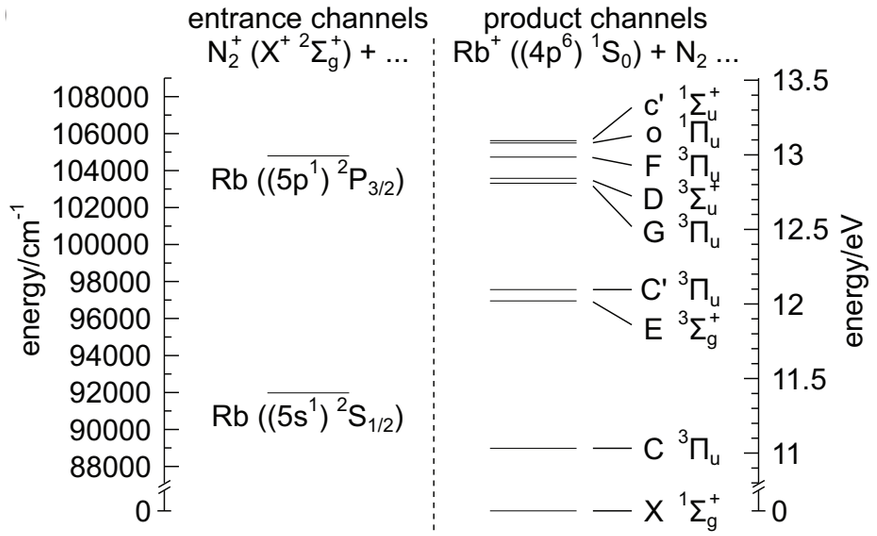

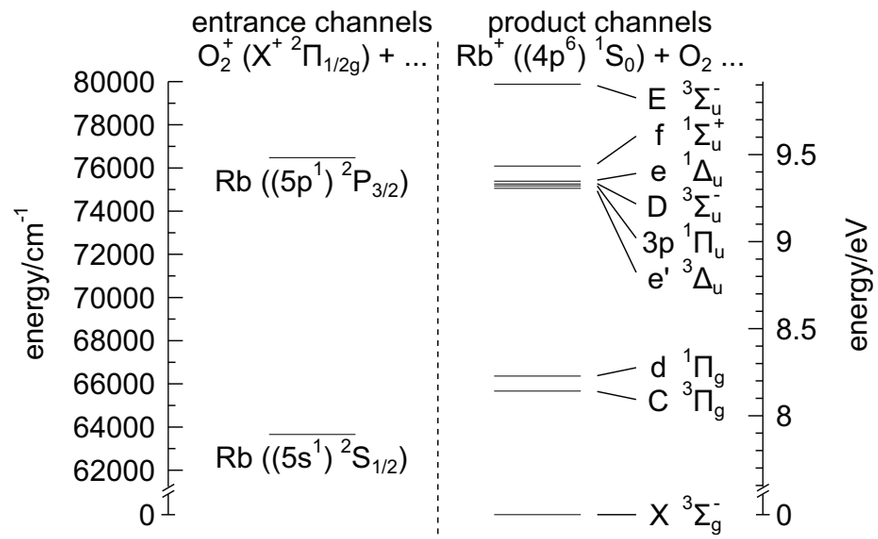

- **Collision-energy dependence of channel-specific rate constants**

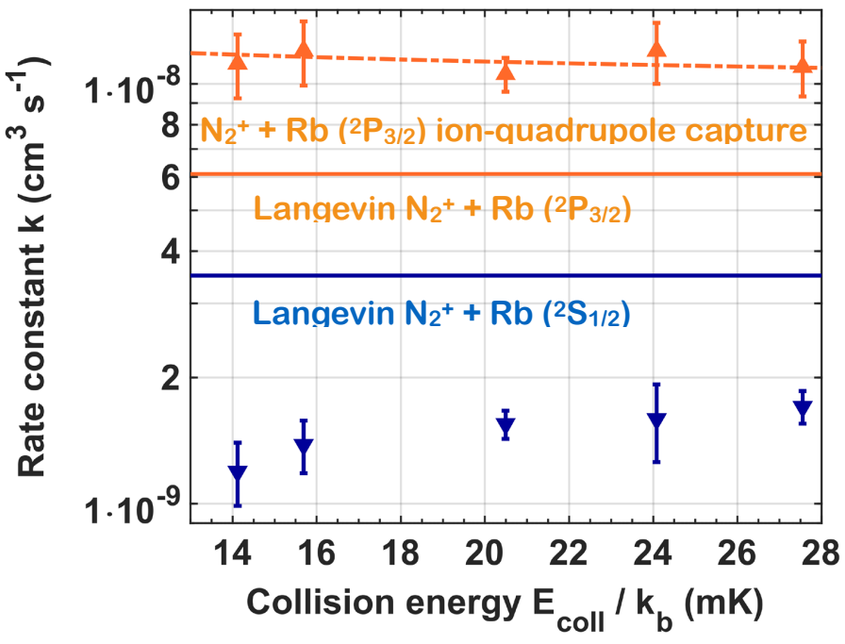

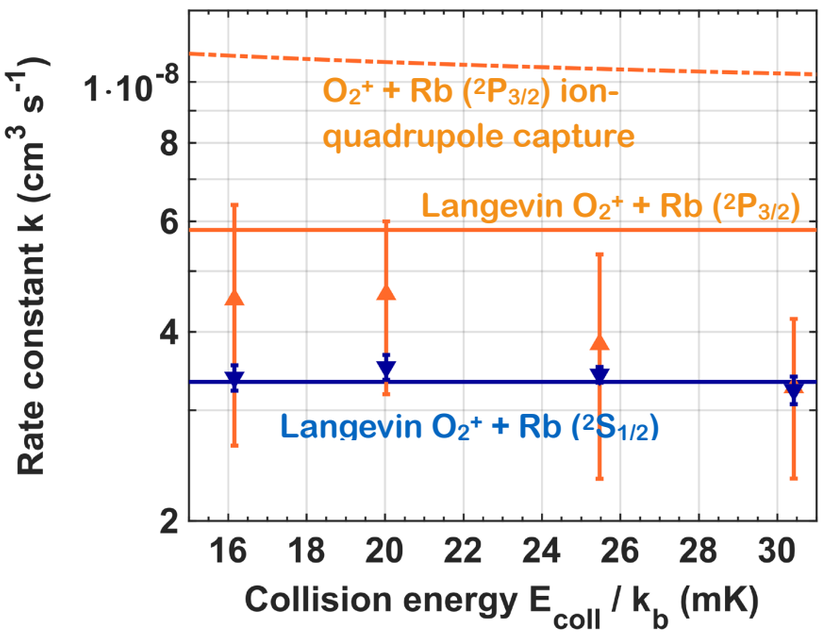

A. D. Dörfler et al., Nat. Commun. 10 (2019), 5429

Charge-transfer dynamics in N_2^+ + Rb ($^2P_{3/2}$):

- The charge-transfer rate constant measured for the excited N_2^+ + Rb ($^2P_{3/2}$) channel at 20mK is $k=2\times10^{-8}$ cm^{3}s^{-1}. Compare with Langevin rate constant for this system: $k_L=6.6\times10^{-9}$ cm^{3}s^{-1}
- Rb in the $^2P_{3/2}$ state exhibits a permanent quadrupole moment. Thus, during the collisions there are charge-quadrupole (CQ) interactions in addition to the charge-induced dipole (CID, Langevin) interactions

Interaction potential: $V(R) = \frac{C_3}{R^3} + \frac{C_4}{R^4}$ (CQ → C_3, CID → C_4)

- The CQ interaction is strongly energy dependent and leads to a considerably increased capture rate constant at very low energies.

Long-range potentials:

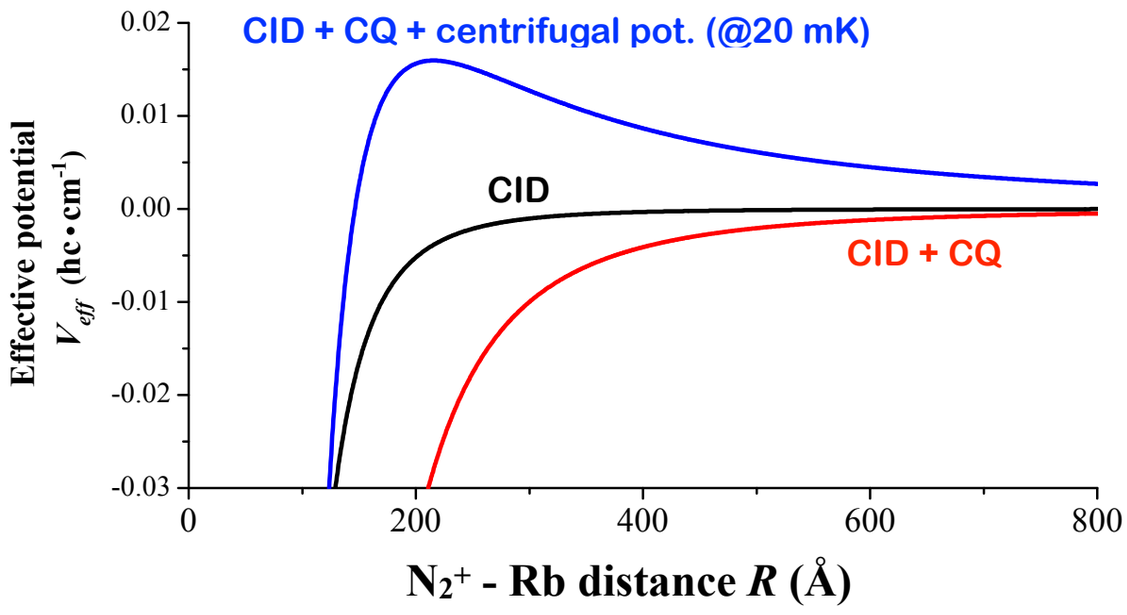

Predicted rate constants:

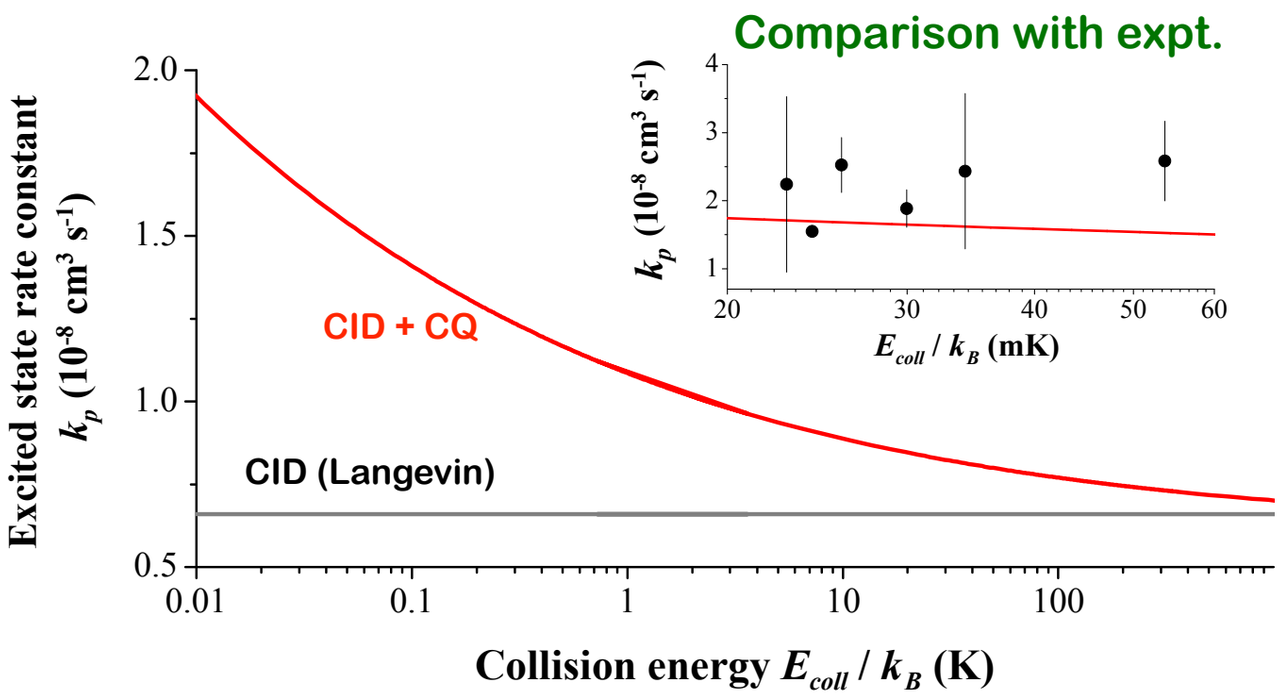

F.H.J. Hall and SW, Phys. Rev. Lett. 109 (2012), 233202; A. D. Dörfler et al., Nat. Commun. 10 (2019), 5429

Charge-transfer dynamics in N_2^+ + Rb ($^2S_{1/2}$):

- In the N_2^+ + Rb ($^2S_{1/2}$) channel, the charge exchange is still fast, but considerably slower than the Langevin rate which would be expected for a capture-limited process in this case
- Thus, short-range effects must play an important role here
- N_2^+ + Rb ($^2S_{1/2}$): angle-dependent potential surface in the triplet channel

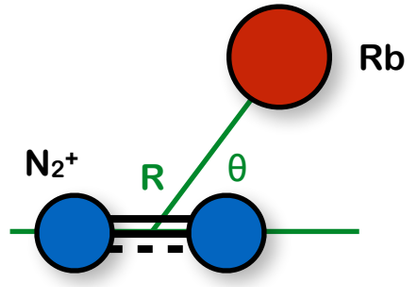

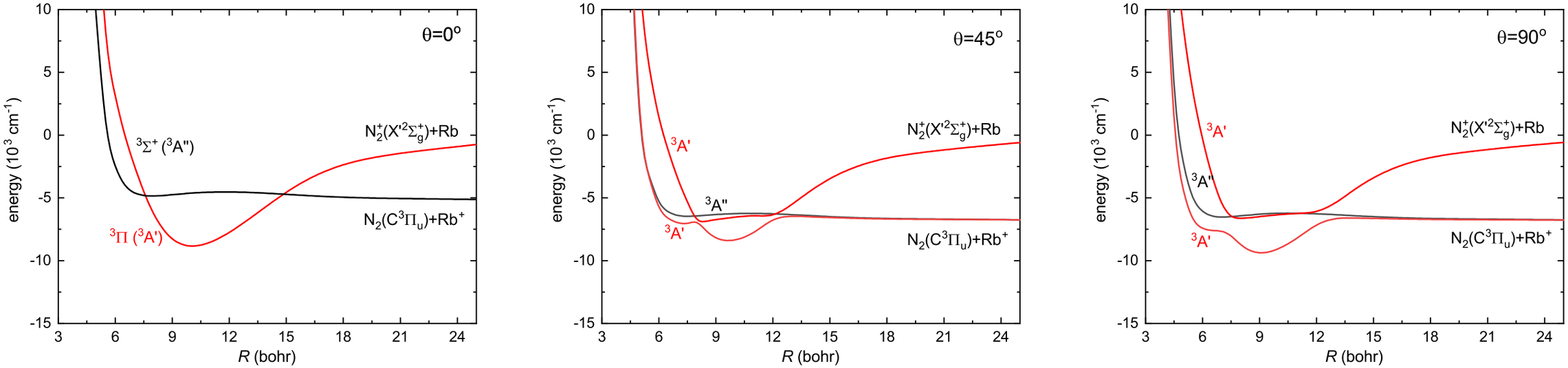

Non-adiabatic charge-transfer occurs around two crossings between potential energy surfaces. The coupling between the surfaces is strongly dependent on the orientation angle θ between N_2^+ and Rb

A. D. Dörfler et al., Nat. Commun. 10 (2019), 5429

- Classical and quantum-dynamics simulations of the collisions reveal a complex collision dynamics with often multiple crossings through the curve crossings (see the trajectory above) and that the charge transfer kinetics is determined by a subtle interplay between long-range and short-range interactions and the detailed topology of the potential-energy surface

- Visualisation of a reactive trajectory

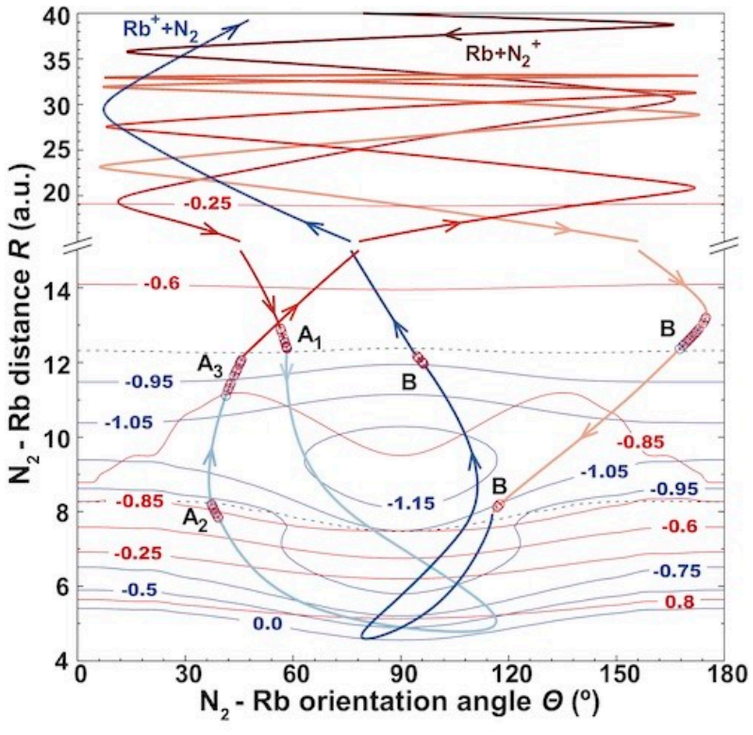

red contour lines:
entrance potential surface
blue contour lines:
charge-transfer potential surface

red/**blue** trajectories indicate motion on the entrance/CT potential surfaces

dashed lines:
crossings between the potential surfaces at which a transition between the surfaces can occur

- Comparison expt. vs. theoretical (quasiclassical and quantum dynamics) charge-transfer rate constants

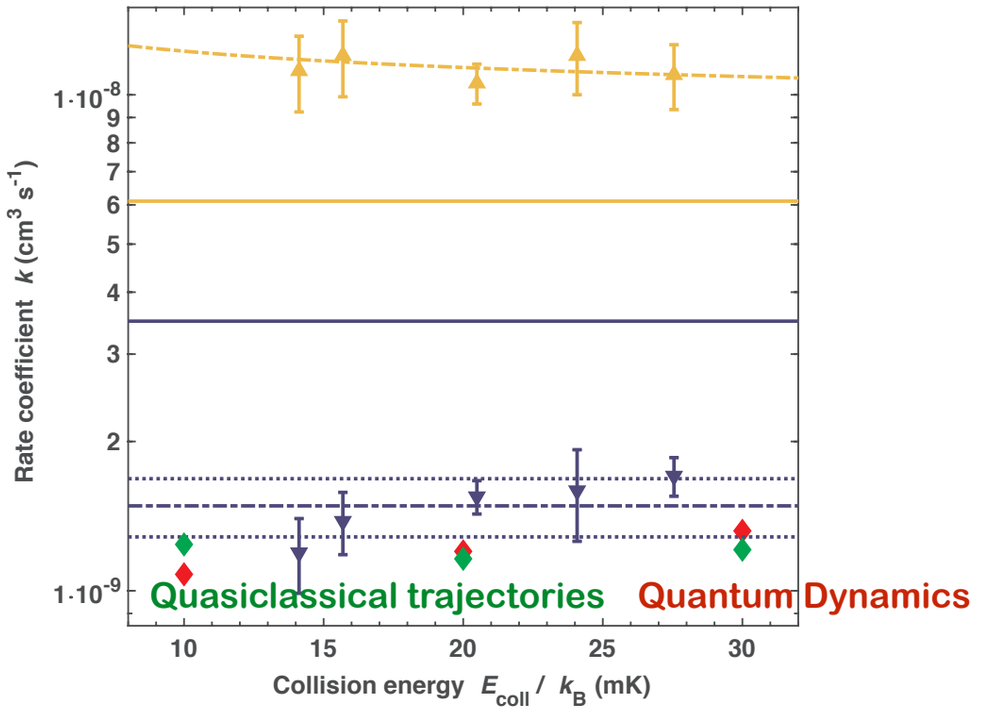

A. D. Dörfler et al., Nat. Commun. 10 (2019), 5429

Synthesis of exotic chemical species in hybrid traps

- The peculiar chemical environment of a hybrid trapping experiment lends itself to the synthesis of exotic chemical compounds which otherwise have so far not been obtainable by other means.
- An example is the synthesis of the mixed hypermetallic oxide $BaOCa^+$ in a Ca-Ba^+ hybrid trap experiment.
- $BaOCa^+$ was obtained in reactions of laser-cooled Ca atoms with $BaOCH_3^+$, which in turn was synthesised from Ba^+ reacting with methanol CH_3OH leaked into the chamber

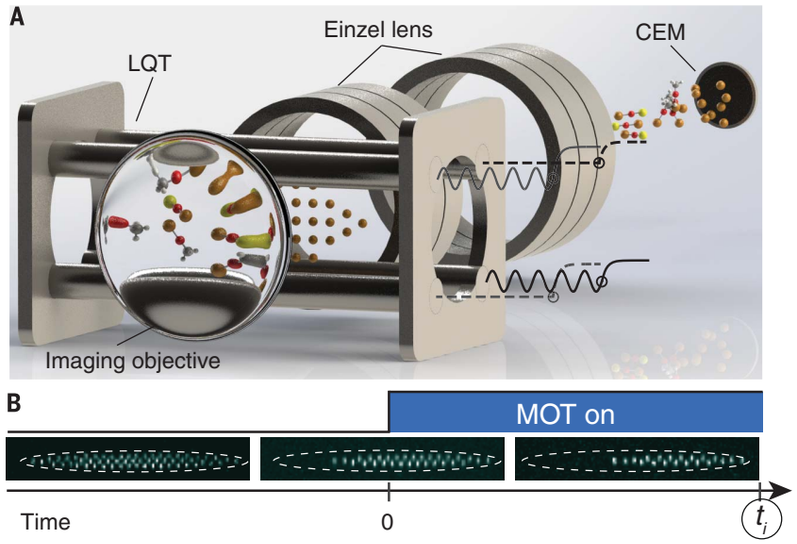

Experiment: A hybrid trap coupled to a time-of-flight mass spectrometer for chemical analysis

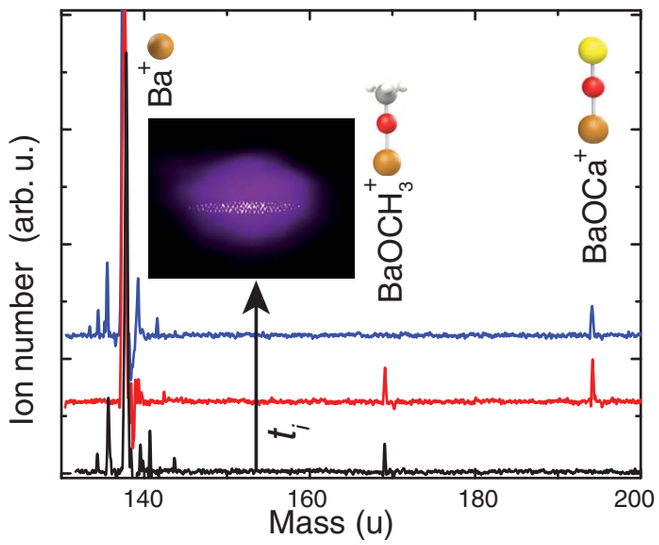

Sample mass spectrum after leaking methanol CH_3OH into the chamber

P. Puri et al., Science 357 (2017), 1370

- Quantum-chemical calculations revealed that the reactions occur with laser-excited Ca ^3P atoms from the MOT with $BaOCH_3^+$ on the excited triplet surface

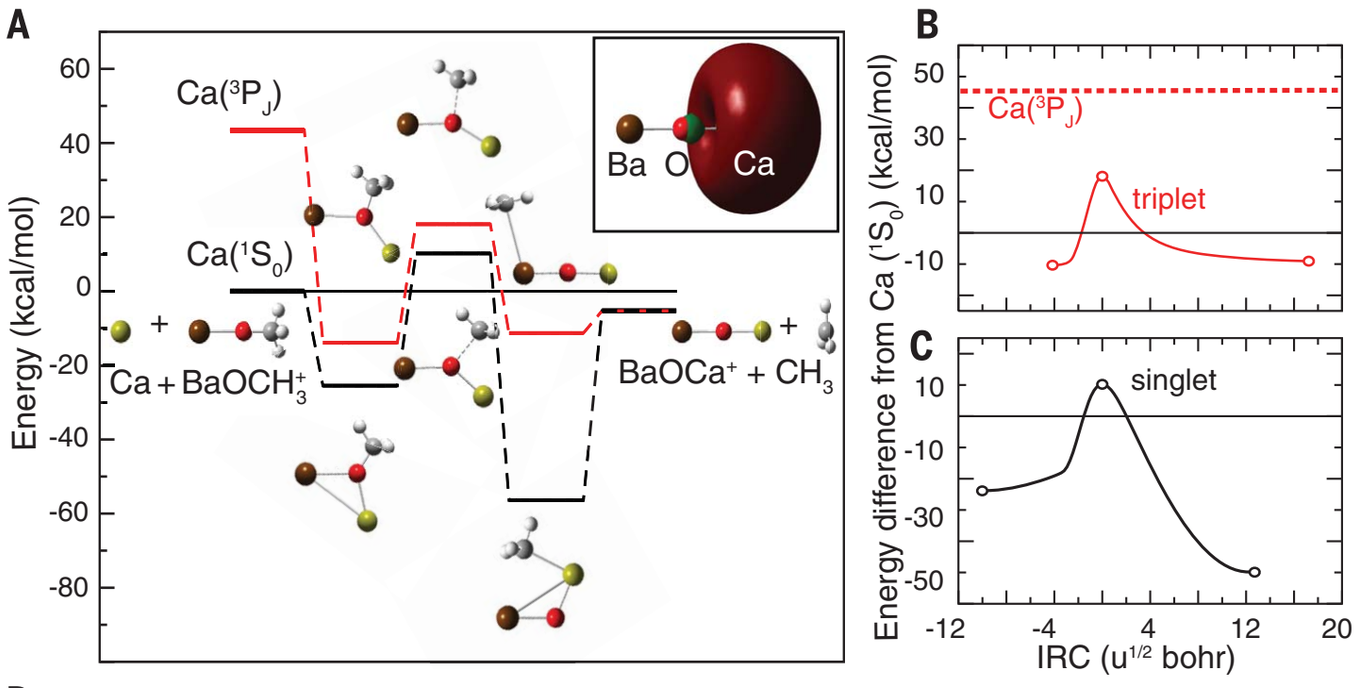

- The hypervalent metal oxide $BaOCa^+$ is of interest to chemists because of its peculiar chemical-bonding characteristics.

P. Puri et al., Science 357 (2017), 1370